



W&M ScholarWorks

Dissertations, Theses, and Masters Projects

Theses, Dissertations, & Master Projects

1985

Fourth order mass splitting in the bag model

Timothy John Havens
College of William & Mary - Arts & Sciences

Follow this and additional works at: <https://scholarworks.wm.edu/etd>

 Part of the [Physics Commons](#)

Recommended Citation

Havens, Timothy John, "Fourth order mass splitting in the bag model" (1985). *Dissertations, Theses, and Masters Projects*. Paper 1539623756.

<https://dx.doi.org/doi:10.21220/s2-3hbt-2b41>

This Dissertation is brought to you for free and open access by the Theses, Dissertations, & Master Projects at W&M ScholarWorks. It has been accepted for inclusion in Dissertations, Theses, and Masters Projects by an authorized administrator of W&M ScholarWorks. For more information, please contact scholarworks@wm.edu.

INFORMATION TO USERS

This reproduction was made from a copy of a document sent to us for microfilming. While the most advanced technology has been used to photograph and reproduce this document, the quality of the reproduction is heavily dependent upon the quality of the material submitted.

The following explanation of techniques is provided to help clarify markings or notations which may appear on this reproduction.

1. The sign or "target" for pages apparently lacking from the document photographed is "Missing Page(s)". If it was possible to obtain the missing page(s) or section, they are spliced into the film along with adjacent pages. This may have necessitated cutting through an image and duplicating adjacent pages to assure complete continuity.
2. When an image on the film is obliterated with a round black mark, it is an indication of either blurred copy because of movement during exposure, duplicate copy, or copyrighted materials that should not have been filmed. For blurred pages, a good image of the page can be found in the adjacent frame. If copyrighted materials were deleted, a target note will appear listing the pages in the adjacent frame.
3. When a map, drawing or chart, etc., is part of the material being photographed, a definite method of "sectioning" the material has been followed. It is customary to begin filming at the upper left hand corner of a large sheet and to continue from left to right in equal sections with small overlaps. If necessary, sectioning is continued again beginning below the first row and continuing on until complete.
4. For illustrations that cannot be satisfactorily reproduced by xerographic means, photographic prints can be purchased at additional cost and inserted into your xerographic copy. These prints are available upon request from the Dissertations Customer Services Department.
5. Some pages in any document may have indistinct print. In all cases the best available copy has been filmed.

**University
Microfilms
International**

300 N. Zeeb Road
Ann Arbor, MI 48106

8526859

Havens, Timothy John

FOURTH ORDER MASS SPLITTING IN THE BAG MODEL

The College of William and Mary in Virginia

PH.D. 1985

University
Microfilms
International

300 N. Zeeb Road, Ann Arbor, MI 48106

PLEASE NOTE:

In all cases this material has been filmed in the best possible way from the available copy. Problems encountered with this document have been identified here with a check mark .

1. Glossy photographs or pages _____
2. Colored illustrations, paper or print _____
3. Photographs with dark background _____
4. Illustrations are poor copy _____
5. Pages with black marks, not original copy _____
6. Print shows through as there is text on both sides of page _____
7. Indistinct, broken or small print on several pages _____
8. Print exceeds margin requirements _____
9. Tightly bound copy with print lost in spine _____
10. Computer printout pages with indistinct print _____
11. Page(s) _____ lacking when material received, and not available from school or author.
12. Page(s) 69 seem to be missing in numbering only as text follows.
13. Two pages numbered 38. Text follows.
14. Curling and wrinkled pages _____
15. Dissertation contains pages with print at a slant, filmed as received _____
16. Other _____

University
Microfilms
International

Fourth Order Mass Splitting In The Bag Model

A dissertation
Presented to
The Faculty of the Department of Physics
The College of William and Mary in Virginia


In Partial Fulfillment
Of the Requirements for the Degree of
Doctor of Philosophy

by
Timothy J. Havens
August 1985

APPROVAL SHEET


This dissertation is submitted in partial fulfillment of
the requirements for the degree of

Doctor of Philosophy



Timothy J. Havens


Approved, August 1985



Carl E. Carlson



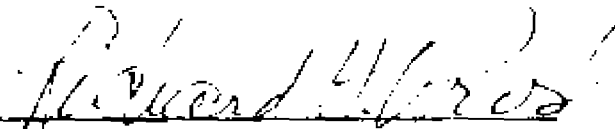
Edward A. Remler



Hans C. von Baeyer



Robert E. Welsh



Richard H. Prosl
(Department of Computer Science)

Dedication

To my parents Harold and Luanne Havens,

my wonderful wife Janine,

and

our son Garrett.

CONTENTS

Dedication	iii
Acknowledgements	v
List of Tables	vi
List of Figures	vii
Abstract	vi

Chapter

I	Introduction	2
II	Extracting the Energy Shift	9
III	Gauge Invariance	20
IV	The Calculation	25
V	Results	46

Appendix

A	Feynman Rules in a static spherical cavity	51
B	Three-j, six-j, and nine-j relations	59
C	The Wick rotation	62
D	Derivation of the coulomb gluon vertex function	65

ACKNOWLEDGEMENTS

I am particularly indebted to the following people for their help and companionship during my stay at William and Mary:

Dr. Carl E. Carlson, my advisor, for his guidance throughout my work with him.

Drs. Robert Siegel, Robert Welsh, John Kane, and Morton Eckhause for their guidance throughout my work with the High Energy Group.

Drs. Carl Carlson, Hans von Baeyer, Robert Welsh, Edward Remler, and Richard Prosi for reading this thesis.

And last, but certainly not least, my friends and colleagues who made my stay at William and Mary a pleasure, especially the Lunch Bunch: Gene Tracy, Saiful Haq, and the lovely Jennifer Poor.

LIST OF TABLES

Table		Page
5-1	Fourth order mass splittings	49

LIST OF FIGURES

Figure		Page
1 a,b	Annihilation diagrams	5
1.c-k	Diagrams in the perturbative expansion	6
2.a	Lowest order diagram	11
2.b	Second order diagram	13
2.c	Fourth order box diagram	16
3.a,b	Coulomb-coulomb box diagrams	21
3.c-e	Mixed coulomb-transverse diagrams	22
4.a-e	Calculated fourth order diagrams	25
4.f,g	Labeling convention for diagrams	27
4.h	Contour choice for Wick rotation	33
A.1	Transverse gluon vertex function	55
A.2	Coulomb gluon vertex function	57
C.1	Contour choice for the Wick rotation	62
D.1	Free field vertex function	66

ABSTRACT

The fourth order diagrams in the perturbative expansion of the hadron mass are calculated using the static spherical cavity approximation to the MIT bag model and Quantum Chromodynamics (QCD). Only terms with color matrix structure different than that of the second order diagrams are retained.

The fourth order mass splitting is found to be smaller than the second order splitting by a factor of three or more.

FOURTH ORDER MASS SPLITTING IN
THE BAG MODEL

CHAPTER I

Introduction

During the 1960's it was found that the large number of newly discovered hadrons could be explained as composites of three elementary particles, the up, down, and strange quarks¹. The possibility of color charge was pointed out by O. W. Greenberg² in 1964, and by 1973 Quantum Chromodynamics³, the hypothesized non-abelian interaction between colored quarks, was in full bloom. This was due largely to the newly found property of asymptotic freedom⁴. Asymptotic freedom is the result that the coupling constant asymptotically approaches a small value for large Q^2 . The QCD running coupling parameter can be expressed as,

$$\alpha(Q^2) = 12\pi / [(33 - 2N_f) \ln(Q^2/\Lambda^2)]$$

where N_f is the number of quark flavors, and Λ is a parameter that must be determined experimentally.

While asymptotic freedom makes perturbative calculations possible at high momentum transfer (small distances), it cannot tell us how the force behaves at small momentum transfer (large distances). The fact

that no colored objects are found in nature indicates that in fact the force is large at large distances, and therefore non-perturbative.

While asymptotic freedom cannot guarantee that the coupling constant is small enough to do perturbative calculations of the hadron mass splittings, the fact that the mass splittings are usually small for a given family of particles indicate that the mass splittings may arise from perturbative aspects of QCD even though the confinement mechanism is non-perturbative.

This was the hope of the group of people at MIT who introduced the bag model⁵. In the MIT bag model the quarks are confined to color singlet hadrons via an infinite square well potential. Inside the hadron they are assumed almost free, the interactions between quarks being those of perturbative QCD.

We consider the static spherical cavity approximation to the MIT bag model. While it is well known that this approximation does not satisfy Lorentz invariance, it is expected that the static hadron properties such as their masses, magnetic moments, and charge radii can be calculated with a considerable degree of confidence. These choices mean the quarks inside the bag are governed by the Dirac equation

$$(i\partial\!\!\!/ - m)\psi(x) = 0$$

for a free particle. The confining potential can be translated into the following boundary condition at the surface of the bag:

$$-i\vec{\gamma} \cdot \vec{\nabla} \psi(x) = \psi(x) \Big|_{x=R}$$

Using the above model the masses of the hadrons have been calculated⁶ to second order in g_C where $g_C^2 = 4\pi\alpha_C$. The result for massless quarks is,

$$M(R) = (4/3)\pi BR^3 - Z_0 R^{-1} + N \omega_0 - .708 \alpha_C (T_1 \cdot T_2) \sum_{i < j} (S_i \cdot S_j) R^{-1}$$

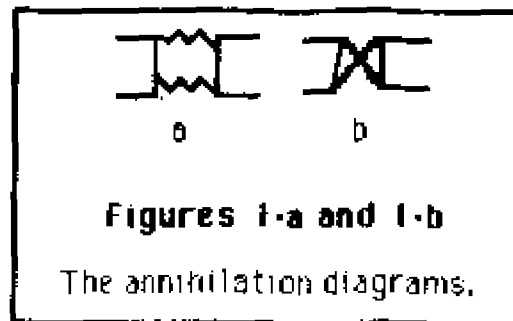
where:

- B = energy density in the bag, $B^{1/4} \approx .145 \text{ GeV}$
- R = radius of bag $\approx .6$ to 1.1 fermi for various hadrons
- $\alpha_C = g_C^2 / 4\pi \approx 2.2$
- Z_0 = zero point energy in the bag ≈ 1.84
- N = number of quarks in the hadron
- ω_0 = energy of quark in 1S state
- $T_1 \cdot T_2$ = color matrices = $-2/3$ for baryons
= $-4/3$ for mesons

B, R, Z_0 and α_C were treated as free parameters and fixed by fitting the above mass formula to the four states N, Δ , p, and Ω . The results for the rest of the spectrum are remarkably good when flavor SU(3) is broken, as can be seen in reference 6. However, there are two main problems with the results. The first problem is that the coupling constant is large. However, since the effective expansion parameter

is $\approx \alpha_c/\pi$, there is still the possibility that the higher order corrections are small.

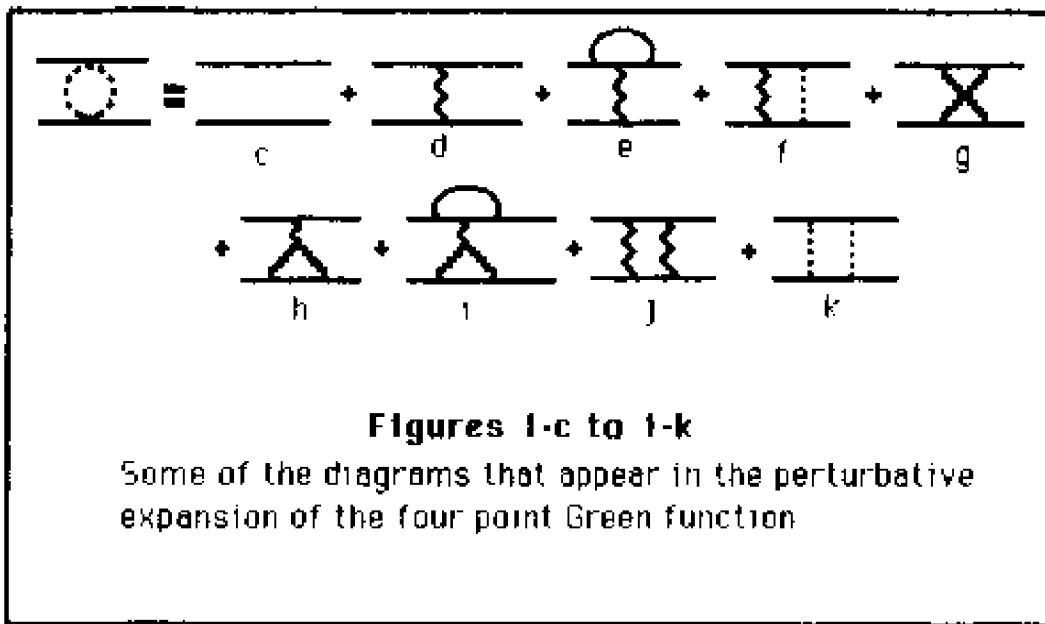
A second problem concerns the $\eta(958)$ - $\eta'(550)$ - $\pi(139)$ mass differences. The mass splitting is partly due to the difference between the strange and the up or down quark masses. However, working only to second order, there will be some linear combination of the η and η' which is degenerate with the π meson. However to fourth order, the isoscalar mesons η and η' have their masses split by the fourth order diagrams shown in Figures 1-a and 1-b.



It had long been observed that if the intermediate states of these diagrams are saturated by the gluonic resonances (glueball(s)), the sign of Figures 1-a and 1-b is determined and makes the η' lighter than the η . The sign argument does not work for a full calculation, mainly due to the possibility of exchanging coulomb gluons. The diagrams were calculated in the coulomb gauge in 1983 by Donahue and Gomm⁷. They found that the sign was right and, with a reasonable α_c the magnitude was right to account for the η - η' mass splitting. This has its disturbing side also, however. The splitting due to these diagrams is

large. This, which is of course connected with the large coupling constant, seriously raises the question of the size of the other fourth order diagrams in the perturbative expansion.

A partial answer to this question is the quest of this thesis. A subset of the diagrams that contribute to the masses of the hadrons are shown in Figures 1-c through 1-k.



A quick glance at the Feynman rules in Appendix A indicate that only diagrams with two gluons exchanged between two quarks have different color matrix structure than that of the second order diagrams. Calculating the fourth order diagrams that have the same color matrix structure as the lower order diagrams would renormalize α_G but would not change the splitting pattern except

under very unusual circumstances. For example, adding the second and fourth order results together we would find an expression like,

$$\Delta E = \alpha_c (N_2 + \alpha_c N_4) T_1 \cdot T_2 + \alpha_c^2 N_4' (T_1 \cdot T_2)^2$$

where N_2 indicates the size of the second order contribution to the energy shifts, N_4 indicates the size of the fourth order contribution with the same color matrix structure, and N_4' indicates the size of the fourth order contribution with different color matrix structure. One can see that the N_4 term will not change the splitting pattern at all, although it can change the fitted value of α_c . Only in the unusual situation that N_4 is much larger than N_4' will it give a more interesting result than N_4' since the latter could qualitatively affect the splitting pattern as well as modify α_c . Thus this thesis concerns itself only with those diagrams that have two gluons exchanged between the two quarks.

The calculation proceeds by a perturbative calculation of the four point Green function. By extracting the pole in the Green function one obtains a perturbative expansion of the mass of the meson. The technique used for doing this is described in Chapter II. A naive calculation of the fourth order diagrams leads to a pinch singularity during the ω integration for parts of the diagram. This problem is also dealt with in Chapter II.

Since we are not calculating the entire set of fourth order

diagrams we must show that the subset we have calculated is gauge invariant by itself. This is discussed in Chapter III. In Chapter IV the relevant diagrams are calculated, and in Chapter V our results are presented.

Appendix A presents the Feynman rules^{8,9} for calculating S-matrix amplitudes. Appendix B lists a number of useful relations between Clebsch-Gordon coefficients¹⁰, three-j symbols, six-j symbols and nine-j symbols.

If the ω integrations associated with the loops in the box and crossed box diagrams were done in the normal way, the residues due to the poles in the propagators would be summed leading to the usual mode sum expressions. Instead, we follow Hansson and Jaffe⁹ and perform the integrals after Wick rotation. To do this we must show that the contributions to the contour integral from the quarter-circles at infinity are zero. This is done in Appendix C.

Finally, to give some feeling of where the Feynman rules of Appendix A came from, the vertex function for the coulomb interaction is loosely derived in Appendix D.

Chapter 11

Extracting The Bound State Energy

In this chapter we examine the pinch singularity that appears in the calculation of the four point Green function. We will show where it appears and why it doesn't enter into the calculation of the bound state energy

While we will use covariant Dirac propagators for the quarks in the actual calculation, we will use only the forward-moving quark part of the mode sum expression for the Dirac propagator in examining the singularity structure of the calculation. We will also ignore all color factors at this time.

To find the energy of the bound quark state we will calculate a projection of the four point Green function,

$$\int [d^4x_i]_{5,8} \bar{u}(x_5) e^{i\omega_5 t_5} \bar{u}(x_6) e^{i\omega_6 t_6}$$

$$\langle\langle 0 | T e^{-iH} | \psi(x_5) \psi(x_6) \bar{\psi}(x_7) \bar{\psi}(x_8) | 0 \rangle\rangle u(x_7) e^{-i\omega_7 t_7} u(x_8) e^{-i\omega_8 t_8}$$

$$\equiv \mathcal{P} \langle\langle 0 | T e^{-iH_I} \psi(x_5) \psi(x_6) \bar{\psi}(x_7) \bar{\psi}(x_8) | 0 \rangle\rangle \equiv -i\Delta$$

where:

$$u(x) \equiv \psi_{1S}(x)$$

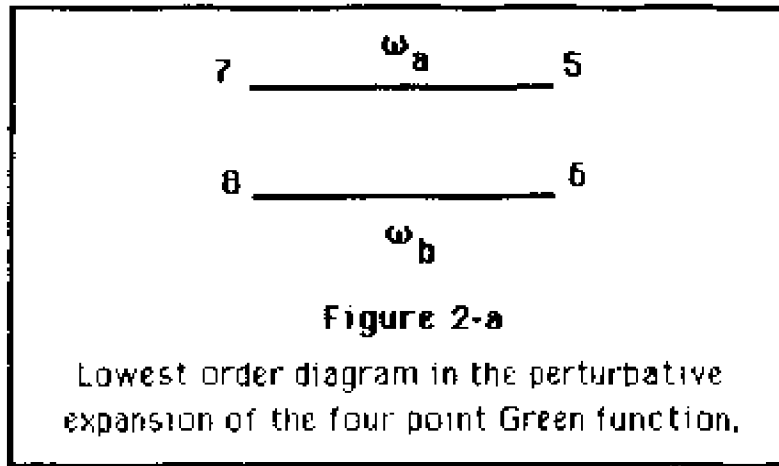
$$\int \{d^4x_i\}_{m,n} \equiv \int d^4x_m d^4x_{m+1} \cdots d^4x_{n-1} d^4x_n$$

unless no subscripts are listed with the box, in which case all x variables are integrated over, and the relevant part of H_I is:

$$H_I = -g_C \int d^4x \bar{\psi}(x) \gamma_\mu \psi(x) A^\mu(x) \equiv \int dt h(x)$$

where $h(x)$ is the Hamiltonian density.

Then to lowest order in perturbation theory we have the following diagram:



Evaluating the relevant projection of the diagram:

$$-i\Delta_0 = P \ll 0 | T \psi(x_5) \psi(x_6) \bar{\psi}(x_7) \bar{\psi}(x_8) | 0 \gg$$

$$= \int [d^4x_i]_{5,8} \bar{u}(x_5) e^{i\omega_5 t_5} \bar{u}(x_6) e^{i\omega_6 t_6}$$

$$i \int d\omega_a e^{-i\omega_a(t_5-t_6)} \sum_m u_m(x_5) u_m(x_7) [2\pi(\omega_a - \omega_m + i\epsilon)]^{-1}$$

$$i \int d\omega_b e^{-i\omega_b(t_6-t_8)} \sum_n u_n(x_6) u_n(x_8) [2\pi(\omega_b - \omega_n + i\epsilon)]^{-1}$$

$$u(x_7) e^{-i\omega_7 t_7} u(x_8) e^{-i\omega_8 t_8}$$

Performing the integrals we find:

$$\Delta_0 = -12\pi\delta(\omega_5 - \omega_7) 2\pi\delta(\omega_6 - \omega_8) [\omega_7 - \omega_0 + i\epsilon]^{-1} [\omega_8 - \omega_0 + i\epsilon]^{-1}$$

To extract the energy of the state let us perform the following integrations:

$$\int d\omega_5 d\omega_6 d\Delta \Delta_{\circ} / (2\pi)^3 = -i \int d\Delta [2\pi(\Omega/2 + \Delta - \omega_{\circ} + i\epsilon)(\Omega/2 - \Delta - \omega_{\circ} + i\epsilon)]^{-1}$$

where:

$$\Delta = (\omega_5 - \omega_6)/2 \quad \text{and} \quad \Omega = (\omega_5 + \omega_6) = \text{total energy}$$

Performing this last integration leaves,

$$\Delta_{\circ} = -[\Omega - 2\omega_{\circ}]^{-1}$$

putting the unperturbed energy at $2\omega_{\circ}$ as expected.

Next let us consider the second order contribution to the four point function:

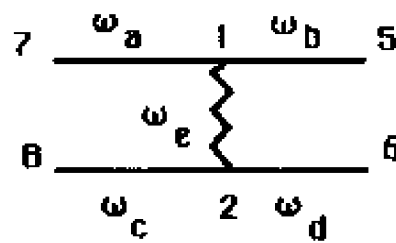


Figure 2-b

Second order diagram in the perturbative expansion of the four point Green function.

$$-i\Delta_2 = P \ll 0 | T : -iH_1(x_1) : : -iH_1(x_2) : \psi(x_5) \bar{\psi}(x_6) \bar{\psi}(x_7) \psi(x_8) | 0 \gg / 2!$$

$$= \int [d^4x_i]_{5,8} \left\{ \bar{u}(x_5) e^{i\omega_5 t_5} \bar{u}(x_6) e^{i\omega_6 t_6} (ig_c)^2 \gamma^\mu_{\alpha\beta} \gamma^\lambda_{\kappa\tau} \right.$$

$$\int d^4x_1 d^4x_2 [i \int (d\omega_e / 2\pi) D_{\mu\lambda}(x_2, x_1, \omega_e) e^{-i\omega_e(t_2 - t_1)}]$$

$$i \int (d\omega_b / 2\pi) e^{-i\omega_b(t_5 - t_1)} \sum_n \bar{u}_n(x_5) \bar{u}_n^\alpha(x_1) (\omega_b - \omega_n + i\epsilon)^{-1}$$

$$i \int (d\omega_a / 2\pi) e^{-i\omega_a(t_1 - t_7)} \sum_m u_m^\beta(x_1) \bar{u}_m(x_7) (\omega_a - \omega_m + i\epsilon)^{-1}$$

$$i \int (d\omega_d / 2\pi) e^{-i\omega_d(t_6 - t_2)} \sum_p u_p(x_6) \bar{u}_p^\kappa(x_2) (\omega_d - \omega_p + i\epsilon)^{-1}$$

$$i \int (d\omega_c / 2\pi) e^{-i\omega_c(t_2 - t_8)} \sum_q u_q^\tau(x_2) \bar{u}_q(x_8) (\omega_c - \omega_q + i\epsilon)^{-1} \left. \right\}$$

$$u(x_7) e^{-i\omega_7 t_7} u(x_8) e^{-i\omega_8 t_8}$$

Doing all of the integrals except those over x_1 and x_2 results in,

$$-i\Delta_2 = 2\pi\delta(\Omega_i - \Omega_f) [(\omega_7 - \omega_0 + i\epsilon)(\omega_8 - \omega_0 + i\epsilon)(\omega_6 - \omega_0 + i\epsilon)(\omega_5 - \omega_0 + i\epsilon)]^{-1}$$

$$\int |d^3x|_{1,2} ((ig_C)u(x_1)\gamma^\mu u(x_1)) iD_{\mu\lambda}(x_2, x_1, \omega_7 - \omega_5) (ig_C)u(x_2)\gamma^\lambda u(x_2)$$

$$= -i 2\pi\delta(\Omega_i - \Omega_f) K_{\omega_0, \omega_0}(\omega_7 - \omega_5)$$

$$[(\omega_7 - \omega_0 + i\epsilon)(\omega_8 - \omega_0 + i\epsilon)(\omega_6 - \omega_0 + i\epsilon)(\omega_5 - \omega_0 + i\epsilon)]^{-1}$$

Now note that the factor in the first line of the above equation is actually the second order S-matrix amplitude for off mass shell quarks,

$$\langle\langle q_5 q_6 | S_2 | q_7 q_8 \rangle\rangle = -i K_{\omega_0, \omega_0}(\omega_7 - \omega_5)$$

The subscripts on $K(\omega)$ indicate the energy state occupied by the quarks on the legs connected to the gluon propagator. To isolate the energy of the bound state we integrate over

$$\Omega_f = \omega_5 + \omega_6, \quad \Delta_i = (\omega_7 - \omega_8)/2, \quad \text{and} \quad \Delta_f = (\omega_5 - \omega_6)/2,$$

ignoring the poles in the gluon propagator. This forces the external

quark legs to the mass shell and gives us the mass of the physical bound quark states.

$$\begin{aligned} \Delta_2 &= i \int (d\Delta_i/2\pi)(d\Delta_f/2\pi) (-iK_{oo,oo}(\Delta_i - \Delta_f)) \\ & (\Omega/2 + \Delta_i - \omega_0 + i\epsilon)(\Omega/2 - \Delta_i - \omega_0 + i\epsilon)(\Omega/2 + \Delta_f - \omega_0 + i\epsilon)(\Omega/2 - \Delta_f - \omega_0 + i\epsilon)^{-1} \\ & = -K_{oo,oo}(0) [\Omega - 2\omega_0]^{-2} = - [\Omega - 2\omega_0]^{-2} i \langle\langle q_5 q_6 | S_2 | q_7 q_8 \rangle\rangle \end{aligned}$$

Or since we are interested in bound states of definite spin, we will be interested in the following S-matrix amplitudes,

$$\Delta_2 = - [\Omega - 2\omega_0]^{-2} i \langle\langle s_1 | S_2 | s_1 \rangle\rangle$$

This implies that to second order,

$$\Delta = \Delta_0 + \Delta_2 = [\Omega - 2\omega_0 + K_{oo,oo}(0)]^{-1}$$

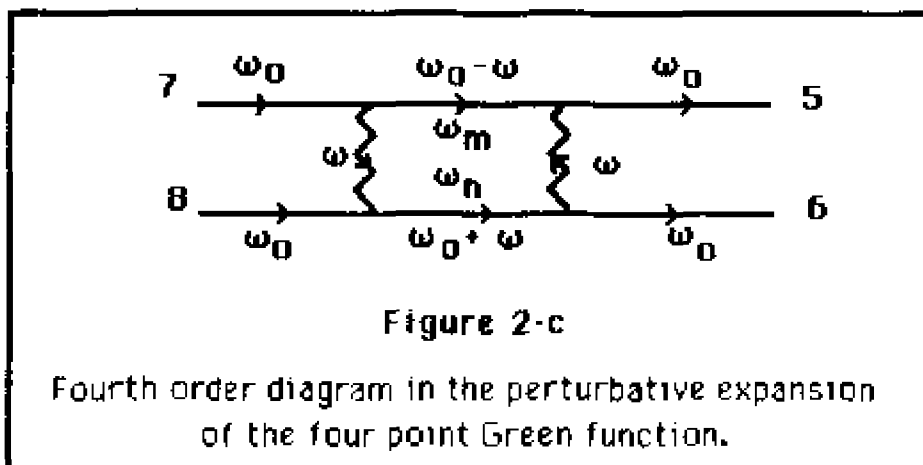
or that the energy of the bound state is at $\Omega = 2\omega_0 - K_{oo,oo}(0)$. Where we have inverted the Green function to extract the energy pole in the standard way. The reader may wish to review the self energy mass

corrections to the electron propagator at this point.

Finally we arrive at the fourth order term. We must calculate

$$\Delta_4 = -[\Omega - 2\omega_0]^{-2} i \langle\langle S_f | S_4 | S_i \rangle\rangle$$

However, only the box diagrams have problems with pinch singularities, so we will only examine the box diagram of Figure 2-c.



$$-i\Delta_4 = -[\Omega - 2\omega_0]^{-2} \langle\langle q_{1S} q_{1S} | S_4 | q_{1S} q_{1S} \rangle\rangle$$

$$\langle\langle q_{1S} q_{1S} | S_4 | q_{1S} q_{1S} \rangle\rangle =$$

$$\begin{aligned}
& (g_c)^4 \int (d\omega/2\pi) \int [d^3x_1]_{1,4} \text{ID}^{\mu\lambda}(x_1, x_3, \omega) \text{ID}^{\kappa\tau}(x_4, x_2, \omega) \\
& \bar{u}(x_3) \gamma_\mu \left[\sum_n u_n(x_3) \bar{u}_n(x_4) [\omega_0 + \omega - \omega_n + i\epsilon]^{-1} \gamma_\lambda u(x_4) \right. \\
& \left. \bar{u}(x_1) \gamma_\kappa \left[\sum_m u_m(x_1) \bar{u}_m(x_2) [\omega_0 - \omega - \omega_m + i\epsilon]^{-1} \gamma_\tau u(x_2) \right. \right.
\end{aligned}$$

Performing the integration over ω we are left with several terms,

$$\begin{aligned}
\langle\langle q_{15} q_{15} | S_4 | q_{15} q_{15} \rangle\rangle &= (g_c)^4 \sum_{m,n} \int [d^3x_1]_{1,4} [2\omega_0 - \omega_m - \omega_n]^{-1} \\
&\text{ID}^{\mu\lambda}(x_1, x_3, \omega_0 - \omega_m) \text{ID}^{\kappa\tau}(x_4, x_2, \omega_0 - \omega_m)
\end{aligned}$$

$$\bar{u}(x_3) \gamma_\mu u_n(x_3) \bar{u}_n(x_4) \gamma_\lambda u(x_4) \bar{u}(x_1) \gamma_\kappa u_m(x_1) \bar{u}_m(x_2) \gamma_\tau u(x_2) + \text{finite}$$

terms from poles in gluon propagator

$$= -i \sum_{m,n} K_{00,mn}(\omega_0 - \omega_m) [2\omega_0 - \omega_m - \omega_n]^{-1} K_{00,mn}(\omega_0 - \omega_m) + \text{finite}$$

terms

Only the first term has any singularity, and that occurs only for that part of the diagram for which the intermediate quark states are the same as the initial states. This part is actually not to be included in the calculation of the energy shift as will be demonstrated below.

Adding the zeroth, second and fourth order results together we find,

$$\Delta = \Delta_0 + \Delta_2 + \Delta_4 = -[\Omega - 2\omega_0]^{-1} - [\Omega - 2\omega_0]^{-2} \left\{ K_{00,00}(0) + \sum_{m,n} K_{00,mn}(\omega_0 - \omega_m) [2\omega_0 - \omega_m - \omega_n]^{-1} K_{00,mn}(\omega_0 - \omega_m) \right\}$$

which can be written as,

$$\Delta = \left[\Omega - 2\omega_0 - K_{00,00}(0) - \sum'_{m,n} K_{00,mn}(\omega_0 - \omega_m) [2\omega_0 - \omega_m - \omega_n]^{-1} K_{00,mn}(\omega_0 - \omega_m) \right]^{-1}$$

where the prime on the summation indicates that the term with intermediate quarks in the same state as the initial quarks is to be excluded. This puts the pole in the total energy at

$$E = 2\omega_0 - K_{00,00}(0) - \sum'_{m,n} K_{00,mn}(\omega_0 - \omega_n) [2\omega_0 - \omega_m - \omega_n]^{-1} K_{00,mn}(\omega_0 - \omega_m) \\ = 2\omega_0 - i \langle\langle S_1 | S_2 | S_1 \rangle\rangle - i \langle\langle S_1 | S_4 | S_1 \rangle\rangle$$

Where the primes have the obvious meaning that the part of the diagram that gives the singularity is to be avoided.

We thus have our prescription for finding the fourth order energy shift of the bound quark states; calculate the fourth order S-matrix element for quarks in a definite spin state but exclude that part of the diagram that is an iteration of the second order diagram. In the actual calculation when we are using covariant Dirac propagators and doing the ω integration after Wick rotation, this will simply mean choosing a contour that excludes the unwanted pole in the Dirac propagator.

Chapter III

Gauge Invariance of The Calculation

As stated in the introduction, since we are not calculating the full set of fourth order Feynman diagrams, we must show that the set of diagrams we have calculated is gauge invariant by itself. We must remember, however, that we are only calculating those diagrams with a certain, $(T_1 \cdot T_2)^2$, color matrix structure. Therefore, we can ignore those parts of the calculated diagrams that result in terms with a different color matrix structure.

The coulomb propagator has a gauge term $\sim \mu/R$. We will show that this term gives zero contribution to the diagrams calculated. For this examination it is again easier to work with the mode sum expansion of the propagator and the normal vertex function used in free field QCD.

First consider the gauge term contribution to the coulomb-coulomb box diagram:

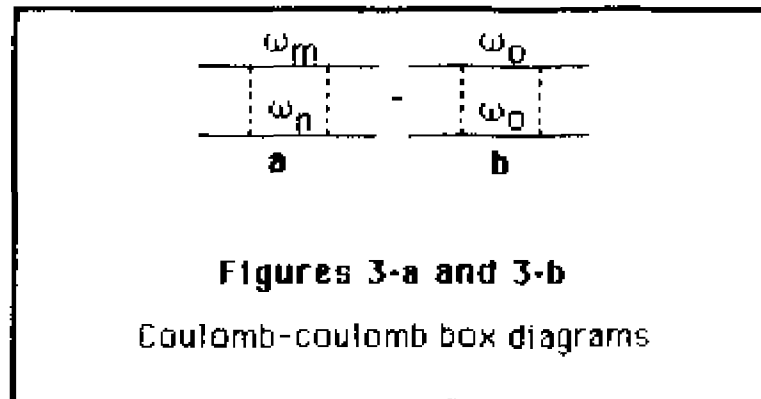


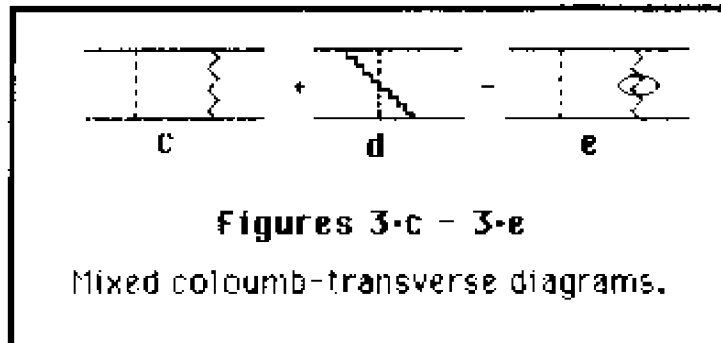
Figure 3.a is the general diagram and Figure 3.b is the iterative piece to be subtracted. Ignoring common factors we find:

$$\begin{aligned}
 a - b \approx & (\mu/R)^2 \int d\omega \int \{d^3x_i\} \\
 & \left\{ \bar{\psi}_{1s}(x_1) \gamma^0 \sum_m (\psi_m(x_1) (\omega_0 - \omega - \omega_m + i\epsilon)^{-1} \bar{\psi}_m(x_2)) \gamma^0 \psi_{1s}(x_2) \right. \\
 & \left. \bar{\psi}_{1s}(x_3) \gamma^0 \sum_n (\psi_n(x_3) (\omega_0 + \omega - \omega_n + i\epsilon) \bar{\psi}_n(x_4)) \gamma^0 \psi_{1s}(x_4) \right\} - \\
 & \left\{ \bar{\psi}_{1s}(x_1) \gamma^0 \psi_{1s}(x_1) (-\omega + i\epsilon)^{-1} \bar{\psi}_{1s}(x_2) \gamma^0 \psi_{1s}(x_2) \right. \\
 & \left. \bar{\psi}_{1s}(x_3) \gamma^0 \psi_{1s}(x_3) (\omega + i\epsilon)^{-1} \bar{\psi}_{1s}(x_4) \gamma^0 \psi_{1s}(x_4) \right\}
 \end{aligned}$$

Since the coulomb gauge term has no x dependence, the integrations

over $x_1, x_2, x_3,$ and x_4 reduce the sum over m and n to only the 1S state. This then cancels the second term giving a total contribution of zero.

Next, consider the mixed coulomb-transverse diagrams.



The wiggly line with a circle on it in Figure 3-e stands for the transverse propagator with $\omega=0$. The last diagram is subtracted because of the pinch singularity discussed in Chapter 2.

$$c+d \approx \mu/R \int d\omega \int [d^3x_i] \left\{ \bar{\psi}_{1S}(x_1) \delta^\mu \sum_m (\psi_m(x_1) (\omega_0 - \omega - \omega_m + i\epsilon)^{-1} \bar{\psi}_m(x_2)) \right. \\ \left. \delta_0 \psi_{1S}(x_2) D_{\mu\lambda}(x_1, x_3, \omega) \right\} \\ \left\{ \bar{\psi}_{1S}(x_3) \delta^\lambda \sum_n (\psi_n(x_3) (\omega_0 + \omega - \omega_n + i\epsilon) \bar{\psi}_n(x_4)) \delta_0 \psi_{1S}(x_4) + \right. \\ \left. \bar{\psi}_{1S}(x_4) \delta_0 \sum_n (\psi_n(x_4) (\omega_0 - \omega - \omega_n + i\epsilon)^{-1} \bar{\psi}_n(x_3)) \delta^\lambda \psi_{1S}(x_3) \right\}$$

Again, since the coulomb gauge term has no x dependence, the

Integrals over x_2 and x_4 constrain the mode sum to include only the 1s state mode. We can thus write:

$$c+d \approx \mu/R \int d\omega \int (d^3x_i) \left\{ \bar{\psi}_{1s}(x_1) \gamma^\mu \psi_{1s}(x_1) (-\omega+i\epsilon)^{-1} \right. \\ \left. \bar{\psi}_{1s}(x_2) \gamma_0 \psi_{1s}(x_2) D_{\mu\lambda}(x_1, x_3, \omega) \right\} \\ \left\{ \bar{\psi}_{1s}(x_3) \gamma^\lambda \psi_{1s}(x_3) (\omega+i\epsilon) \bar{\psi}_{1s}(x_4) \gamma_0 \psi_{1s}(x_4) + \right. \\ \left. \bar{\psi}_{1s}(x_3) \gamma^\lambda \psi_{1s}(x_3) \bar{\psi}_{1s}(x_4) \gamma_0 \psi_{1s}(x_4) (-\omega+i\epsilon)^{-1} \right\}$$

The x dependence is the same in both terms so let us ignore it and examine the ω dependence only:

$$c+d \approx \int d\omega (-\omega+i\epsilon)^{-1} D(\omega) \{ (\omega+i\epsilon)^{-1} + (-\omega+i\epsilon)^{-1} \}$$

There are poles in $D(\omega)$ but the quantity in curly brackets assures their residues give no contribution. This leaves the pole at $\omega=0$ with which to contend. If we close the integral in the upper half plane, the second term in curly brackets gives zero contribution. Pulling the contribution from diagram *e* back into the picture, we are left with the residue at $\omega=0$ for the following integral:

$$b+c-d \approx \int d\omega (-\omega+i\epsilon)^{-1} (\omega+i\epsilon)^{-1} \{ D(\omega) - D(0) \}$$

which is zero.

This completes the proof that the calculation is gauge invariant under the restricted gauge transformation $G(x) \approx G(x) + \mu/R$. We believe that since the above diagrams are the only ones with the above color matrix structure, we can be reasonably certain that they are gauge invariant by themselves.

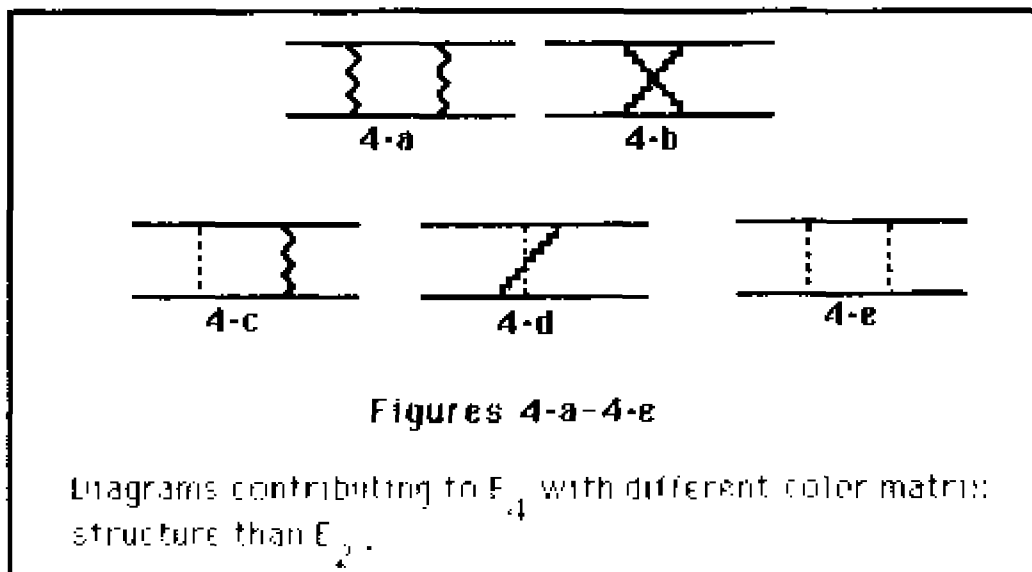
Chapter IV

The calculation

As shown in Chapter II, the fourth order energy contribution is given by,

$$E_4 = i \langle\langle S_f | S_4' | S_i \rangle\rangle$$

where, again, the prime on S_4 indicates we do not include the pinch singularity at $\omega=0$. Also as stated previously, we will only calculate those S-matrix amplitudes that have a different color matrix structure than that of the second order contribution. The diagrams corresponding to these amplitudes are shown in Figures 4-a through 4-e.



To calculate these diagrams first expand the S-matrix amplitude:

$$\langle\langle s_f | s | s_i \rangle\rangle = \sum_{\mu_1, \mu_2, \mu_3, \mu_4}$$

$$\langle\langle s_f \mu | s_1 \mu_1, s_3 \mu_3 \rangle\rangle \langle\langle s_1 \mu_1, s_3 \mu_3 | s | s_2 \mu_2, s_4 \mu_4 \rangle\rangle$$

$$\langle\langle s_2 \mu_2, s_4 \mu_4 | s_1 \mu_1 \rangle\rangle$$

Use of equation B-1 results in:

$$\langle\langle s_f | s | s_i \rangle\rangle = \sum_{\mu_1, \mu_2, \mu_3, \mu_4} (-1)^{s_3 - s_1 - \mu_1 + s_4 - s_2 - \mu_1} \\ [(2s_f + 1)(2s_i + 1)]^{1/2}$$

$$\begin{pmatrix} s_1 & s_3 & s_f \\ \mu_1 & \mu_3 & \mu_f \end{pmatrix} \begin{pmatrix} s_2 & s_4 & s_i \\ \mu_2 & \mu_4 & \mu_i \end{pmatrix} \langle\langle s_1 \mu_1, s_3 \mu_3 | s | s_2 \mu_2, s_4 \mu_4 \rangle\rangle$$

We can now evaluate the above matrix element using the Feynman rules listed in Appendix A. A box and crossed box diagram are shown in more detail with all necessary labeling in Figures 4-f and 4-g. The dashed lines represent either coulomb or transverse gluons. The same labeling will be used for all five diagrams whether the exchanged gluons are transverse or coulomb.

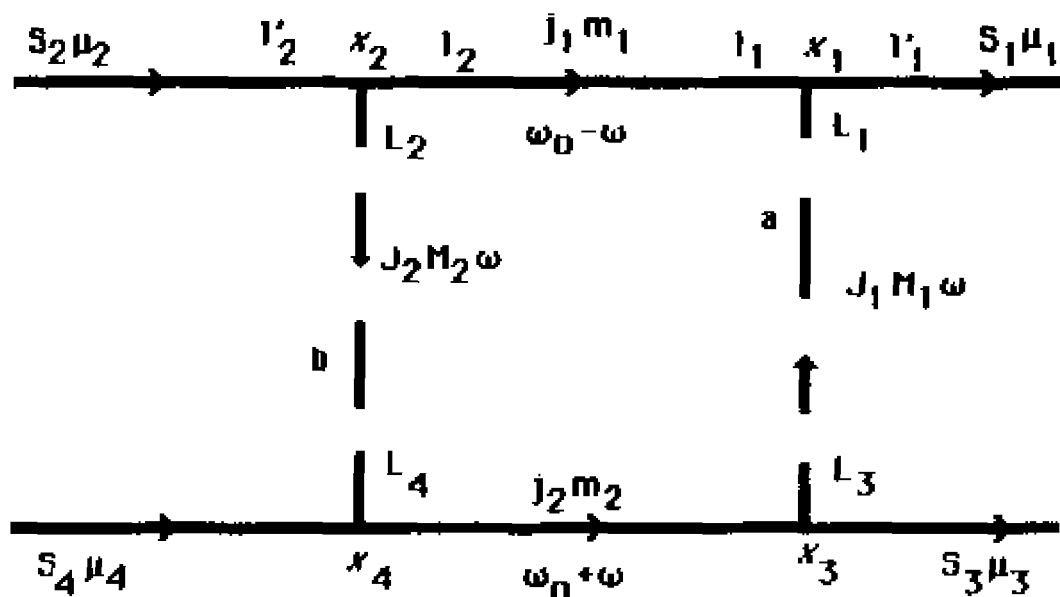


Figure 4-f

Labeling convention for box diagrams.

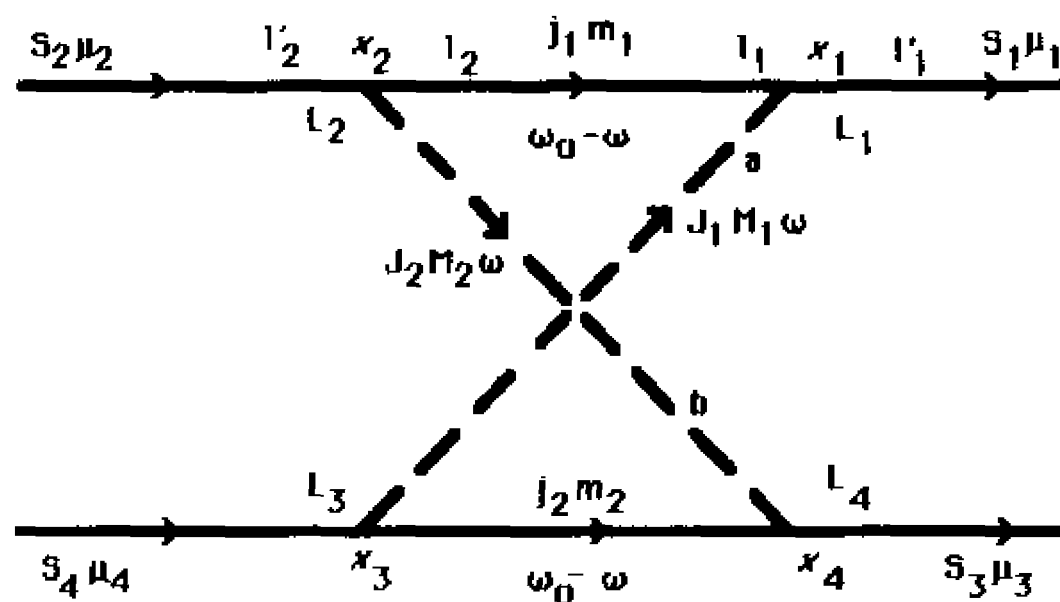


Figure 4-g

Labeling convention for crossed box diagrams.

We make the following definition:

$$E_4 \equiv \text{TTBOX} + \text{CTBOX} + \text{CCBOX} + \text{TTCROSS} + \text{CTCROSS}$$

Where the prefixes TT, CT, and CC have the obvious definitions:

TT≡transverse-transverse, CT≡coulomb-transverse, and
CC≡coulomb-coulomb.

Consider first the box diagram with two transverse gluons. Use of the Feynman Rules in Appendix A results in:

$$\text{TTBOX} \equiv \sum_{\mu_1, \mu_2, \mu_3, \mu_4} (-1)^{S_3 - S_1 - \mu_f + S_4 - S_2 - \mu_i} \\ \left[(2S_f + 1)(2S_i + 1) \right]^{1/2} \\ \begin{pmatrix} S_1 & S_3 & S_f \\ \mu_1 & \mu_3 & \mu_f \end{pmatrix} \begin{pmatrix} S_2 & S_4 & S_i \\ \mu_2 & \mu_4 & \mu_i \end{pmatrix}$$

$$i \langle\langle S_1 \mu_1, S_3 \mu_3 | S_f \mu_f | S_2 \mu_2, S_4 \mu_4 \rangle\rangle$$

$$\text{TTBOX} = ig_c^4 (T_1 \cdot T_2)^2 \int d\omega / 2\pi \int [dx_i |x_i|^2]$$

$$\langle \chi_{l_1 m_1}(x_1) | l_1 1/2 \quad 1/2 | | Y_{j_1 l_1 \sigma} \rangle | l_1 1/2 \quad j_1 \rangle$$

$$\rho^2 S_{j_1 l_1 l_2}(x_1, x_2, \omega_0 - \omega) \rho^2 \left(l_2 \ 1/2 \ j_1 \ \parallel \ Y_{J_2 L_2} \cdot \sigma \ \parallel \ l_2 \ 1/2 \ 1/2 \right) \\ \chi_{l_2}(x_2) \left[\chi_{l_3}(x_3) \left(l_3 \ 1/2 \ 1/2 \ \parallel \ Y_{J_1 L_3} \cdot \sigma \ \parallel \ l_3 \ 1/2 \ j_2 \right) \right. \\ \left. \rho^2 S_{j_2 l_3 l_4}(x_3, x_4, \omega_0 + \omega) \rho^2 \right. \\ \left. \left(l_4 \ 1/2 \ j_2 \ \parallel \ Y_{J_2 L_4} \cdot \sigma \ \parallel \ l_4 \ 1/2 \ 1/2 \right) \chi_{l_4}(x_4) \right] D_{J_1 L_1 L_3}(x_1, x_3, \omega) \\ D_{J_2 L_4 L_2}(x_4, x_2, \omega)$$

$$\sum_{\text{all } m, M, \mu} (-1)^{l_1 + l_2 + J_1 + J_2 - (m_1 + m_2 + M_1 + M_2 + \mu_r + \mu_l + \mu_1 + \mu_3) - L_2 - L_3 - 1} \\ \begin{pmatrix} S_1 & S_3 & S_r \\ \mu_1 & \mu_3 & -\mu_r \end{pmatrix} \begin{pmatrix} S_1 & J_1 & l_1 \\ -\mu_1 & M_1 & m_1 \end{pmatrix} \begin{pmatrix} S_3 & J_1 & l_2 \\ -\mu_3 & -M_1 & m_2 \end{pmatrix} \begin{pmatrix} S_2 & S_4 & S_l \\ \mu_2 & \mu_4 & -\mu_l \end{pmatrix} \\ \begin{pmatrix} S_2 & l_1 & J_2 \\ \mu_2 & -m_1 & -M_2 \end{pmatrix} \begin{pmatrix} S_4 & l_2 & J_2 \\ \mu_4 & -m_2 & M_2 \end{pmatrix} \left[(2S_l + 1)(2S_r + 1) \right]^{1/2}$$

Notice that only the three-j symbols depend upon the z component of angular momentum. We shall denote this summation *Spin Sum* and evaluate it next.

We split the sum into two parts and use the three-j relations in appendix B :

$$\text{Spin Sum} = (-1)^{l_1 + l_2 + J_1 + J_2 + (\mu_r - m_1 - m_2) - L_2 - L_3 - 1}$$

$$\sum_{\mu_1, M_1, \mu_3} (-1)^{M_1 + \mu_1 + \mu_3 + J_1 + S_1 + j_1}$$

$$\begin{pmatrix} S_1 & S_1 & S_3 \\ -\mu_1 & \mu_1 & \mu_3 \end{pmatrix} \begin{pmatrix} J_1 & j_2 & S_3 \\ -M_1 & m_2 & -\mu_3 \end{pmatrix} \begin{pmatrix} J_1 & S_1 & j_1 \\ M_1 & -\mu_1 & m_1 \end{pmatrix}$$

$$\sum_{\mu_2, \mu_4, M_2} (-1)^{\mu_2 + \mu_4 + M_2 + j_1 + S_2 + J_2}$$

$$\begin{pmatrix} S_4 & S_2 & S_1 \\ -\mu_4 & -\mu_2 & \mu_1 \end{pmatrix} \begin{pmatrix} J_1 & S_2 & J_2 \\ -m_1 & \mu_2 & -M_2 \end{pmatrix} \begin{pmatrix} S_4 & j_2 & J_2 \\ \mu_4 & -m_2 & M_2 \end{pmatrix}$$

Next let μ_3 go to $-\mu_3$ in the first sum, and let μ_4 go to $-\mu_4$ in the second sum. This results in:

$$\text{Spin sum} = (-1)^{j_1 + j_2 - L_2 - L_3 - 1} \sum_{m_1, m_2} (-1)^{(\mu_1 - m_1 - m_2)}$$

$$\sum_{\mu_1, M_1, \mu_3} (-1)^{M_1 + \mu_1 + \mu_3}$$

$$\begin{pmatrix} S_1 & S_1 & S_3 \\ -\mu_1 & \mu_1 & -\mu_3 \end{pmatrix} \begin{pmatrix} J_1 & j_2 & S_3 \\ -M_1 & m_2 & \mu_3 \end{pmatrix} \begin{pmatrix} J_1 & S_1 & j_1 \\ M_1 & -\mu_1 & m_1 \end{pmatrix}$$

$$\sum_{\mu_2, \mu_4, M_2} (-1)^{\mu_2 + \mu_4 + M_2}$$

$$\begin{pmatrix} S_4 & S_2 & S_i \\ \mu_4 & -\mu_2 & \mu_i \end{pmatrix} \begin{pmatrix} j_1 & S_2 & J_2 \\ -m_1 & \mu_2 & -M_2 \end{pmatrix} \begin{pmatrix} S_4 & j_2 & J_2 \\ -\mu_4 & -m_2 & M_2 \end{pmatrix}$$

Use of B-3 results in:

$$\text{Spin sum} = \sum_{m_1, m_2} (-1)^{j_1 + j_2 + J_1 + J_2 + (\mu_f - m_1 - m_2) - L_2 - L_3 - 1}$$

$$\begin{pmatrix} j_1 & j_2 & S_f \\ m_1 & m_2 & -\mu_f \end{pmatrix} \begin{pmatrix} j_1 & j_2 & S_i \\ -m_1 & -m_2 & \mu_i \end{pmatrix} \left\{ \begin{matrix} j_1 & j_2 & S_f \\ 1/2 & 1/2 & J_1 \end{matrix} \right\} \left\{ \begin{matrix} j_1 & j_2 & S_i \\ 1/2 & 1/2 & J_2 \end{matrix} \right\}$$

Noting $\mu_f = m_1 + m_2$ and using B-2 we arrive at our final form for the spin sum:

$$\text{Spin sum} = (-1)^{j_1 + j_2 + J_1 + J_2 - L_2 - L_3 - 1} \delta_{S_i, S_f} \delta_{\mu_i, \mu_f} (2S_f + 1)^{-1}$$

$$\left\{ \begin{matrix} j_1 & j_2 & S_f \\ 1/2 & 1/2 & J_1 \end{matrix} \right\} \left\{ \begin{matrix} j_1 & j_2 & S_i \\ 1/2 & 1/2 & J_2 \end{matrix} \right\}$$

Which allows us to write:

$$\text{TTBOX} = i g_c^4 (T_1 \cdot T_2)^2 \int d\omega / 2\pi \int [dx_i \kappa_i^2]$$

$$\begin{aligned}
& \{ \chi_{l_1} (x_1) (l_1 \ 1/2 \ 1/2 \ || Y_{J_1 L_1} \sigma || l_1 \ 1/2 \ j_1) \\
& \rho^2 S_{j_1 l_1 l_2} (x_1, x_2, \omega_0 - \omega) \rho^2 (l_2 \ 1/2 \ j_1 \ || Y_{J_2 L_2} \sigma || l_2 \ 1/2 \ 1/2) \\
& \chi_{l_2} (x_2) \} \{ \chi_{l_3} (x_3) (l_3 \ 1/2 \ 1/2 \ || Y_{J_3 L_3} \sigma || l_3 \ 1/2 \ j_2) \rho^2 \\
& S_{j_2 l_3 l_4} (x_3, x_4, \omega_0 + \omega) \rho^2 \\
& (l_4 \ 1/2 \ j_2 \ || Y_{J_4 L_4} \sigma || l_4 \ 1/2 \ 1/2) \chi_{l_4} (x_4) \} D_{J_1 L_1 L_3} (x_1, x_3, \omega) \\
& D_{J_2 L_2 L_4} (x_4, x_2, \omega) (-1)^{l_1 + l_2 + J_1 + J_2 - L_2 - L_3 - 1}
\end{aligned}$$

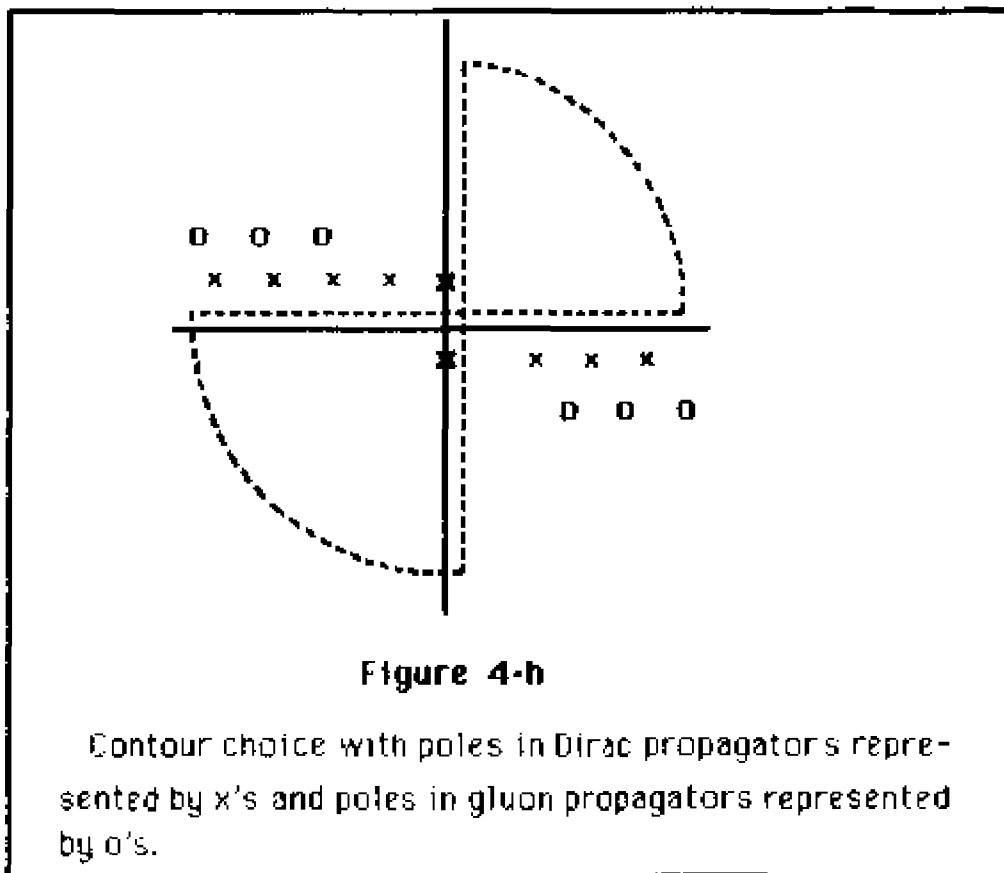
$$\left\{ \begin{matrix} l_1 & l_2 & s \\ 1/2 & 1/2 & J_1 \end{matrix} \right\} \left\{ \begin{matrix} l_1 & l_2 & s \\ 1/2 & 1/2 & J_2 \end{matrix} \right\}$$

At this point we could perform the ω integration along the real ω axis. This would pick up the poles in the propagators and produce the mode sum expressions used in chapters II and III. Instead, we will rotate the contour and replace the slowly convergent mode sums with a rapidly convergent integration parallel to the imaginary ω axis. To do this we must verify that the two quarter-circles at infinity give zero contribution to the desired integral. This will be shown in appendix D.

We are interested in evaluating TTBOX:

$$\text{TTBOX} = i \int (d\omega/2\pi) F(\omega) - \text{Residue}[F(\omega=0)]$$

Consider the integral around the contour in the complex ω plane shown in figure 4-h.



The pinch singularity comes from the poles in the Dirac propagator shown on the imaginary ω axis. The above contour eliminates the unwanted term that has the singularity as will be shown below.

Now integrate around the dashed contour shown in Figure 4-h:

$$i \oint (dz/2\pi) F(z) = \text{Residue}[F(\omega=0)]$$

$$= i \int_{-\infty}^{\infty} (d\omega/2\pi) F(\omega) + i \int_{c+i\infty}^c (dz/2\pi) F(z) + \text{zero terms}$$

which implies that,

$$\text{TTBOX} = -i \int_{c+i\infty}^c (dz/2\pi) F(z)$$

Letting $z=c-i\eta$ we obtain,

$$\text{TTBOX} = - \int_{-\infty}^{\infty} (d\eta/2\pi) F(c-i\eta)$$

$$= -g_c^4 (T_1 \cdot T_2)^2 \int d\eta/2\pi \int (dx_i x_i^2)$$

$$\{ \chi_{1'1}(x_1) (l_1^{1/2} \quad 1/2 \quad || Y_{J_1 L_1} \cdot \sigma || l_1^{1/2} \quad j_1)$$

$$\rho^2 S_{j_1 l_1 l_2}(x_1, x_2, \omega_0 - z) \rho^2 (l_2^{1/2} \quad j_1 \quad || Y_{J_2 L_2} \cdot \sigma || l_2^{1/2} \quad 1/2) \chi_{1'2}(x_2) \}$$

$$\{ \chi_{1'3}(x_3) (l_3^{1/2} \quad 1/2 \quad || Y_{J_1 L_3} \cdot \sigma || l_3^{1/2} \quad j_2) \rho^2 S_{j_2 l_3 l_4}(x_3, x_4, \omega_0 + z) \rho^2$$

$$(l_4^{1/2} \quad j_2 \quad || Y_{J_2 L_4} \cdot \sigma || l_4^{1/2} \quad 1/2) \chi_{1'4}(x_4) \} D_{J_1 L_1 L_3}(x_1, x_3, z)$$

$$D_{J_2 L_2 L_2}(x_4, x_2, z) (-1)^{j_1 + j_2 + J_1 + J_2 - L_2 - L_3 - 1}$$

$$\left\{ \begin{matrix} j_1 & j_2 & S \\ 1/2 & 1/2 & J_1 \end{matrix} \right\} \quad \left\{ \begin{matrix} j_1 & j_2 & S \\ 1/2 & 1/2 & J_2 \end{matrix} \right\}$$

This is our final analytic expression and must be evaluated numerically.

Next consider the box diagram with two coulomb gluons being exchanged. Use of the Feynman rules in Appendix A result in:

$$\begin{aligned} \text{CCBOX} = & i g_c^4 (T_1 \cdot T_2)^2 \int d\omega / 2\pi \int |dx_i x_i^2| \\ & \{ \chi_{1'1}(x_1) (l_1 \ 1/2 \ 1/2 || Y_{J_1} || l_1 \ 1/2 \ j_1) \\ & \rho^3 S_{j_1 l_1 l_2}(x_1, x_2, \omega_0 - \omega) \rho^3 (l_2 \ 1/2 \ j_1 || Y_{J_2} || l_2 \ 1/2 \ 1/2) \chi_{1'2}(x_2) \} \\ & \{ \chi_{1'3}(x_3) (l_3 \ 1/2 \ 1/2 || Y_{J_1} || l_3 \ 1/2 \ j_2) \rho^3 S_{j_2 l_3 l_4}(x_3, x_4, \omega_0 + \omega) \rho^3 \\ & (l_4 \ 1/2 \ j_2 || Y_{J_2} || l_4 \ 1/2 \ 1/2) \chi_{1'4}(x_4) \} G_{J_1}(x_1, x_3) \\ & G_{J_2}(x_4, x_2) [(2s_1 + 1)(2s_1 + 1)]^{1/2} \\ & \sum_{\text{all } m, M, \mu} (-1)^{j_1 + j_2 - (m_1 + m_2 + M_1 + M_2 + \mu_1 + \mu_2 + \mu_3) + 1} \end{aligned}$$

$$\begin{pmatrix} S_1 & S_3 & S_f \\ \mu_1 & \mu_3 & -\mu_f \end{pmatrix} \begin{pmatrix} S_1 & J_1 & J_1 \\ -\mu_1 & M_1 & m_1 \end{pmatrix} \begin{pmatrix} S_3 & J_1 & J_2 \\ -\mu_3 & -M_1 & m_2 \end{pmatrix} \begin{pmatrix} S_2 & S_4 & S_i \\ \mu_2 & \mu_4 & -\mu_i \end{pmatrix} \begin{pmatrix} S_2 & J_1 & J_2 \\ \mu_2 & -m_1 & -M_2 \end{pmatrix} \quad 36$$

$$\begin{pmatrix} S_4 & J_2 & J_2 \\ \mu_4 & -m_2 & M_2 \end{pmatrix}$$

Notice that the sum over the z component of angular momentum is the same as *Spin Sum* in the evaluation of TTBOX except for a factor

$$(-1)^{J_1+J_2-L_2-L_3}$$

We can thus write:

$$\text{ccbox Spin Sum} = (-1)^{J_1+J_2+1} \delta_{S_i, S_f} \delta_{\mu_i, \mu_f} (2S_f+1)^{-1}$$

$$\left\{ \begin{matrix} J_1 & J_2 & S_f \\ 1/2 & 1/2 & J_1 \end{matrix} \right\} \left\{ \begin{matrix} J_1 & J_2 & S_i \\ 1/2 & 1/2 & J_2 \end{matrix} \right\}$$

Performing a Wick rotation as in the TTBOX calculation, we arrive at our final analytic expression for CCBOX.

$$\begin{aligned}
\text{CCBOX} = & -g_c^4 (T_1 \cdot T_2)^2 \int d\eta / 2\pi \int (dx_1 x_1^2) \\
& \{ \chi_{l_1'}(x_1) (l_1' \ 1/2 \ 1/2 \ || \ Y_{J_1} \ || \ l_1 \ 1/2 \ j_1) \\
& \rho^3 S_{j_1 l_1 l_1 l_2}(x_1, x_2, \omega_0 - z) \rho^3 (l_2 \ 1/2 \ j_1 \ || \ Y_{J_2} \ || \ l_2' \ 1/2 \ 1/2) \chi_{l_2'}(x_2) \} \\
& \{ \chi_{l_3'}(x_3) (l_3' \ 1/2 \ 1/2 \ || \ Y_{J_1} \ || \ l_3 \ 1/2 \ j_2) \rho^3 S_{j_2 l_3 l_3 l_4}(x_3, x_4, \omega_0 + z) \rho^3 \\
& (l_4 \ 1/2 \ j_2 \ || \ Y_{J_2} \ || \ l_4' \ 1/2 \ 1/2) \chi_{l_4'}(x_4) \} G_{J_1}(x_1, x_3) \\
& G_{J_2}(x_4, x_2) (-1)^{l_1 + j_2 + 1}
\end{aligned}$$

$$\left\{ \begin{matrix} j_1 & j_2 & s \\ 1/2 & 1/2 & J_1 \end{matrix} \right\} \left\{ \begin{matrix} j_1 & j_2 & s \\ 1/2 & 1/2 & J_2 \end{matrix} \right\}$$

Next consider the box diagram with one coulomb gluon and one transverse gluon being exchanged. Use of the Feynman rules in Appendix A result in:

$$\begin{aligned}
 \text{CTBOX} = & -g_c^4 (T_1 \cdot T_2)^2 \int d\omega/2\pi \int [dx_i x_i^2] \\
 & \{ \chi_{1'1}(x_1) (l_1' 1/2 \ 1/2 || Y_{J_1 L_1} \cdot \sigma || l_1' 1/2 \ j_1) \\
 & \rho^2 S_{j_1 l_1 l_2}(x_1, x_2, \omega_0 - \omega) \rho^3 (l_2 1/2 \ j_1 || Y_{J_2} || l_2' 1/2 \ 1/2) \chi_{1'2}(x_2) \} \\
 & \{ \chi_{1'3}(x_3) (l_3' 1/2 \ 1/2 || Y_{J_1 L_3} \cdot \sigma || l_3' 1/2 \ j_2) \rho^2 S_{j_2 l_3 l_4}(x_3, x_4, \omega_0 + \omega) \\
 & \rho^3 (l_4 1/2 \ j_2 || Y_{J_2} || l_4' 1/2 \ 1/2) \chi_{1'4}(x_4) \} D_{J_1 L_1 L_3}(x_1, x_3, \omega) \\
 & G_{J_2}(x_4, x_2) [(2S_i + 1)(2S_f + 1)]^{1/2} \\
 & \sum_{\text{all } m, M, \mu} (-1)^{j_1 + j_2 + j_1 - (m_1 + m_2 + M_1 + M_2 + \mu_f + \mu_i + \mu_1 + \mu_3) - L_3} \\
 & \begin{pmatrix} S_1 & S_3 & S_f \\ \mu_f & \mu_3 & -\mu_f \end{pmatrix} \begin{pmatrix} S_1 & j_1 & j_1 \\ -\mu_1 & m_1 & m_1 \end{pmatrix} \begin{pmatrix} S_3 & j_1 & j_2 \\ -\mu_3 & -m_1 & m_2 \end{pmatrix} \begin{pmatrix} S_2 & S_4 & S_i \\ \mu_2 & \mu_4 & -\mu_i \end{pmatrix} \begin{pmatrix} S_2 & j_1 & j_2 \\ \mu_2 & -m_1 & -M_2 \end{pmatrix} \\
 & \begin{pmatrix} S_4 & j_2 & j_2 \\ \mu_4 & -m_2 & M_2 \end{pmatrix}
 \end{aligned}$$

Notice that the sum over the z component of angular momentum is the same as *Spin Sum* in the evaluation of TTBOX except for a factor $(-1)^{J_2-L_2-1}$.

We can thus write:

$$\text{ctbox Spin Sum} = (-1)^{J_1+J_2+J_1-L_3} (2S_f+1)^{-1}$$

$$\left\{ \begin{matrix} j_1 & j_2 & S \\ 1/2 & 1/2 & J_1 \end{matrix} \right\} \left\{ \begin{matrix} j_1 & j_2 & S \\ 1/2 & 1/2 & J_2 \end{matrix} \right\}$$

This allows us to write our final analytic expression for CTBOX.

$$\begin{aligned} \text{CTBOX} = & -g_c^4 (T_1 \cdot T_2)^2 \int d\eta/2\pi \int [dx_i x_i^2] \\ & \{ \chi_{1'1}(x_1, \omega_1) \chi_{1'2}(x_2, \omega_2) \chi_{1'3}(x_3) \chi_{1'4}(x_4) \} \\ & \rho^2 S_{j_1 j_1 j_2}(x_1, x_2, \omega_0 - z) \rho^3 (j_2 \ 1/2 \ j_1 \ || \ Y_{J_2} \ || \ j_2 \ 1/2 \ 1/2) \chi_{1'2}(x_2) \\ & \dots \\ & (\chi_{1'3}(x_3) (j_3 \ 1/2 \ 1/2 \ || \ Y_{J_1 L_3} \ || \ j_3 \ 1/2 \ j_2) \rho^2 S_{j_2 j_3 j_4}(x_3, x_4, \omega_0 + z) \\ & \rho^3 (j_4 \ 1/2 \ j_2 \ || \ Y_{J_2} \ || \ j_4 \ 1/2 \ 1/2) \chi_{1'4}(x_4)) D_{J_1 L_1 L_3}(x_1, x_3, \omega) \\ & G_{J_2}(x_4, x_2) (-1)^{J_1+J_2+J_1+L_3+1} \end{aligned}$$

$$\left\{ \begin{matrix} j_1 & j_2 & S \\ 1/2 & 1/2 & J_1 \end{matrix} \right\} \left\{ \begin{matrix} j_1 & j_2 & S \\ 1/2 & 1/2 & J_2 \end{matrix} \right\}$$

Next let us find an analytic expression for the crossed box in which both gluons are transverse.

$$\begin{aligned}
 T_{\text{CROSS}} &= ig_c^4 (T_1 \cdot T_2)^2 \int d\omega/2\pi \int (dx_1 x_1^2) \\
 &\quad \{ \chi_{1'1}(x_1) (1'1 \ 1/2 \ 1/2 \ || Y_{J_1 L_1} \sigma \ || 1'1 \ 1/2 \ j_1) \\
 &\quad \rho^2 S_{j_1 | 1'1 1/2}(x_1, x_2, \omega_0 - \omega) \rho^2 (1'2 \ 1/2 \ j_1 \ || Y_{J_2 L_2} \sigma \ || 1'2 \ 1/2 \ 1/2) \\
 &\quad \chi_{1'2}(x_2) \} \{ \chi_{1'4}(x_4) (1'4 \ 1/2 \ 1/2 \ || Y_{J_2 L_4} \cdot \sigma \ || 1'4 \ 1/2 \ j_2) \rho^2 S_{j_2 | 1'4 1/2} \\
 &\quad (x_4, x_3, \omega_0 - \omega) \rho^2 (1'3 \ 1/2 \ j_2 \ || Y_{J_1 L_3} \cdot \sigma \ || 1'3 \ 1/2 \ 1/2) \chi_{1'3}(x_3) \} \\
 &\quad D_{J_1 L_1 L_3}(x_1, x_3, \omega) \quad D_{J_2 L_4 L_2}(x_4, x_2, \omega) \\
 &\quad \sum_{\text{all } m, M, \mu} (-1)^{j_1 + j_2 + J_1 + J_2 - (m_1 + m_2 + M_1 + M_2 + \mu_1 + \mu_2 + \mu_3 + \mu_4) - L_2 - L_3 - 1} \\
 &\quad \begin{pmatrix} S_1 & S_3 & S_f \\ \mu_1 & \mu_3 & -\mu_f \end{pmatrix} \begin{pmatrix} S_1 & J_1 & j_1 \\ -\mu_1 & M_1 & m_1 \end{pmatrix} \begin{pmatrix} S_3 & J_2 & j_2 \\ -\mu_3 & M_2 & m_2 \end{pmatrix} \begin{pmatrix} S_2 & S_4 & S_i \\ \mu_2 & \mu_4 & -\mu_i \end{pmatrix} \begin{pmatrix} S_2 & j_1 & j_2 \\ \mu_2 & -m_1 & -M_2 \end{pmatrix} \\
 &\quad \begin{pmatrix} S_4 & j_2 & J_1 \\ \mu_4 & -m_2 & -M_1 \end{pmatrix} \quad [(2S_i + 1)(2S_f + 1)]^{1/2}
 \end{aligned}$$

We again concentrate only on the summation over the z component of angular momentum. We shall denote this summation *Cross Spin Sum*

and evaluate it next. Noting that $S_i = S_f$ and $\mu_i = \mu_f$, and taking advantage of the rotational invariance of the problem we can sum on μ_i if we divide by $(2S+1)$.

$$\text{Cross Spin Sum} = (-1)^{j_1 + j_2 + J_1 + J_2 - L_2 - L_3 - 1} (2S + 1)^{-1}$$

$$\sum_{\mu_1, \mu_2, \mu_3, \mu_4, m_1, m_2, M_1, M_2} (-1)^{(m_1 + m_2 + M_1 + M_2 + \mu_f + \mu_i + \mu_1 + \mu_3)}$$

$$\begin{pmatrix} S_1 & S_3 & S_f \\ \mu_1 & \mu_3 & -\mu_f \end{pmatrix} \begin{pmatrix} S_1 & J_1 & J_1 \\ -\mu_1 & M_1 & m_1 \end{pmatrix} \begin{pmatrix} S_3 & J_2 & J_2 \\ -\mu_3 & M_2 & m_2 \end{pmatrix}$$

$$\begin{pmatrix} S_2 & S_4 & S_i \\ \mu_2 & \mu_4 & -\mu_i \end{pmatrix} \begin{pmatrix} S_2 & J_1 & J_2 \\ \mu_2 & -m_1 & -M_2 \end{pmatrix} \begin{pmatrix} S_4 & J_2 & J_1 \\ \mu_4 & -m_2 & -M_1 \end{pmatrix}$$

To use expression **B-4** we must note that $m_1 + m_2 + M_1 + M_2 + \mu_f + \mu_i + \mu_1 + \mu_3$ is always even and can thus be discarded from the exponent. We must also make all the lower components of the three-j symbols positive. We do this by letting $\mu_1, \mu_2, \mu_3, \mu_4$ go into their negatives, then changing the sign of the lower components of some of the resulting three-j symbols. This will be done in two steps.

$$\text{Cross Spin Sum} = (-1)^{j_1 + j_2 + J_1 + J_2 - L_2 - L_3 - 1} (2S + 1)^{-1}$$

$$\sum_{\mu_1, \mu_2, \mu_3, \mu_4, \mu, m_1, m_2, M_1, M_2} \begin{pmatrix} S_1 & S_3 & S_f \\ -\mu_1 & -\mu_3 & -\mu_f \end{pmatrix} \begin{pmatrix} S_1 & J_1 & j_1 \\ \mu_1 & M_1 & m_1 \end{pmatrix} \begin{pmatrix} S_3 & J_2 & j_2 \\ \mu_3 & M_2 & m_2 \end{pmatrix}$$

$$\begin{pmatrix} S_2 & S_4 & S_i \\ -\mu_2 & -\mu_4 & -\mu_i \end{pmatrix} \begin{pmatrix} S_2 & j_1 & J_2 \\ -\mu_2 & -m_1 & -M_2 \end{pmatrix} \begin{pmatrix} S_4 & j_2 & J_1 \\ -\mu_4 & -m_2 & -M_1 \end{pmatrix}$$

Now change the signs in lower components.

$$\text{Cross Spin Sum} = (-1)^{j_1 + j_2 + J_1 + J_2 - L_2 - L_3 - 1} (2S + 1)^{-1} (-1)^{j_1 + j_2 + S}$$

$$\sum_{\mu_1, \mu_2, \mu_3, \mu_4, \mu, m_1, m_2, M_1, M_2} \begin{pmatrix} S_1 & S_3 & S_f \\ \mu_1 & \mu_3 & \mu_f \end{pmatrix} \begin{pmatrix} J_1 & j_2 & S_4 \\ M_1 & m_2 & \mu_4 \end{pmatrix} \begin{pmatrix} j_1 & J_2 & S_2 \\ m_1 & M_2 & \mu_2 \end{pmatrix}$$

$$\begin{pmatrix} S_1 & J_1 & j_1 \\ \mu_1 & M_1 & m_1 \end{pmatrix} \begin{pmatrix} S_3 & j_2 & J_2 \\ \mu_3 & m_2 & M_2 \end{pmatrix} \begin{pmatrix} S_i & S_4 & S_2 \\ \mu_i & \mu_4 & \mu_2 \end{pmatrix}$$

Therefore, using **B-4**

$$\text{Cross Spin Sum} = (-1)^{S+J_1+J_2-L_2-L_3-1} (2S+1)^{-1}$$

$$\left\{ \begin{array}{ccc} S_1 & S_3 & S_1 \\ J_1 & J_2 & S_4 \\ J_1 & J_2 & S_2 \end{array} \right\}$$

Using the symmetry properties of the nine-j symbol we can rewrite this as

$$\text{Cross Spin Sum} = (-1)^{J_1+J_2+L_2+L_3+1} (2S+1)^{-1}$$

$$\left\{ \begin{array}{ccc} S_1 & S_3 & S_1 \\ J_1 & J_1 & S_4 \\ J_2 & J_2 & S_2 \end{array} \right\}$$

Thus our final expression after Wick rotation for TTCROSS is,

$$\text{TTCROSS} = -g_c^4 (T_1 \cdot T_2)^2 \int d\eta / 2\pi \int [dx_i x_i^2]$$

$$\{ \chi_{l_1}(x_1) (l_1 \ 1/2 \ 1/2 \ || \ Y_{J_1 L_1} \cdot \sigma \ || \ l_1 \ 1/2 \ j_1)$$

$$\rho^2 S_{j_1 l_1 l_2}(x_1, x_2, \omega_0 - z) \rho^2 (l_2 \ 1/2 \ j_1 \ || \ Y_{J_2 L_2} \cdot \sigma \ || \ l_2 \ 1/2 \ 1/2) \chi_{l_2}(x_2) \}$$

$$\{ \chi_{l_4}(x_4) (l_4 \ 1/2 \ 1/2 \ || \ Y_{J_4 L_4} \cdot \sigma \ || \ l_4 \ 1/2 \ j_2) \rho^2 S_{j_2 l_4 l_3}(x_4, x_3, \omega_0 - z) \rho^2$$

$$(l_3 \ 1/2 \ j_2 \ || \ Y_{J_3 L_3} \cdot \sigma \ || \ l_3 \ 1/2 \ 1/2) \chi_{l_3}(x_3) \} D_{J_1 L_1 l_1 j_1}(x_1, x_3, z)$$

$$D_{J_2 L_2 l_2 j_2}(x_4, x_2, z) (-1)^{J_1+J_2+L_2+L_3+1}$$

$$\left\{ \begin{array}{l} S_1 \quad S_3 \quad S_f \\ j_1 \quad J_1 \quad S_4 \\ J_2 \quad j_2 \quad S_2 \end{array} \right\}$$

where again, $z=c-i\eta$.

And finally we evaluate the expression for the last diagram, that of the crossed box diagram in which one gluon is transverse and one is coulomb.

$$\begin{aligned} \text{CTCROSS} &= ig_c^4 (T_1 \cdot T_2)^2 \int d\omega/2\pi \int [dx_i x_i^2] \\ &\quad \{ \chi_{l_1}(x_1) (l_1 \ 1/2 \ 1/2 \ || \ Y_{J_1 L_1} \cdot \sigma \ || \ l_1 \ 1/2 \ j_1) \\ &\quad \rho^2 S_{j_1 l_1 l_2}(x_1, x_2, \omega_0 - \omega) \rho^3 (l_2 \ 1/2 \ j_1 \ || \ Y_{J_2} \ || \ l_2 \ 1/2 \ 1/2) \chi_{l_2}(x_2) \} \\ &\quad \{ \chi_{l_4}(x_4) (l_4 \ 1/2 \ 1/2 \ || \ Y_{J_2} \ || \ l_4 \ 1/2 \ j_2) \rho^3 S_{j_2 l_4 l_3}(x_4, x_3, \omega_0 - \omega) \rho^2 \\ &\quad (l_3 \ 1/2 \ j_2 \ || \ Y_{J_1 L_3} \cdot \sigma \ || \ l_3 \ 1/2 \ 1/2) \chi_{l_3}(x_3) \} D_{J_1 L_1 L_3}(x_1, x_3, \omega) \\ &\quad G_{J_2}(x_4, x_2) \quad [(2S_1 + 1)(2S_f + 1)]^{1/2} \\ &\quad \sum_{\text{all } m_i, \mu_i} (-1)^{j_1 + j_2 + J_1 - (m_1 + m_2 + M_1 + M_2 + \mu_1 + \mu_2 + \mu_3) - L_3 + 1} \end{aligned}$$

$$\begin{pmatrix} S_1 & S_3 & S_f \\ \mu_1 & \mu_3 & -\mu_f \end{pmatrix} \begin{pmatrix} S_1 & J_1 & j_1 \\ -\mu_1 & M_1 & m_1 \end{pmatrix} \begin{pmatrix} S_3 & J_2 & l_2 \\ -\mu_3 & M_2 & m_2 \end{pmatrix} \begin{pmatrix} S_2 & S_4 & S_i \\ \mu_2 & \mu_4 & -\mu_i \end{pmatrix} \begin{pmatrix} S_2 & j_1 & J_2 \\ \mu_2 & -m_1 & -M_2 \end{pmatrix}$$

$$\begin{pmatrix} S_4 & l_2 & J_1 \\ \mu_4 & -m_2 & M_1 \end{pmatrix}$$

This time the summation over the z component of angular momentum is the same as *Cross Spin Sum* in the TTCROSS calculation except for a factor:

$$(-1)^{J_2 - L_2}$$

Therefore,

$$\text{ctcross Spin Sum} = (-1)^{j_1 + j_2 + J_2 + L_3 + 1} (2S + 1)^{-1}$$

$$\begin{Bmatrix} S_1 & S_3 & S_f \\ j_1 & j_1 & S_4 \\ J_2 & l_2 & S_2 \end{Bmatrix}$$

And our final expression for CTCROSS is:

$$\text{CTCROSS} = -g_c^4 (T_1 \cdot T_2)^2 \int d\eta / 2\pi \int [dx_1 x_1^2]$$

$$\{ \chi_{l_1} (x_1) (l_1 \pm 1/2 \pm 1/2) \} \{ Y_{J_1 L_1} \cdot \sigma \} \{ l_1 \pm 1/2 j_1 \}$$

$$\begin{aligned}
 & \rho^2 S_{j_1 l_1 l_2}(x_1, x_2, \omega_0 - z) \rho^3 (l_2 \ 1/2 \ j_1 \ || \ Y_{j_2} \ || \ l'_2 \ 1/2 \ 1/2) \chi_{l'_2}(x_2) \} \\
 & \{ \chi_{l'_4}(x_4) (l'_4 \ 1/2 \ 1/2 \ || \ Y_{j_2} \ || \ l_4 \ 1/2 \ j_2) \rho^3 S_{j_2 l_4 l_3}(x_4, x_3, \omega_0 - z) \rho^2 \\
 & (l_3 \ 1/2 \ j_2 \ || \ Y_{j_1 l_3 - \sigma} \ || \ l'_3 \ 1/2 \ 1/2) \chi_{l'_3}(x_3) \} D_{j_1 l_1 l_3}(x_1, x_3, z) \\
 & G_{j_2}(x_4, x_2) (-1)^{j_1 + j_2 + j_2 + l_3 + l}
 \end{aligned}$$

$$\left\{ \begin{array}{ccc} s_1 & s_3 & s_1 \\ j_1 & j_1 & s_4 \\ j_2 & j_2 & s_2 \end{array} \right\}$$

This concludes the analytic portion of the calculation. The final expressions listed for each diagram are then evaluated numerically. The integration is done via a Monte Carlo integration program developed by G. C. Sheppey.

Chapter V

Results and Summary

The final analytic expressions for the various diagrams were calculated numerically for the case in which $j_1 = j_2 = 1/2$ only. A study of the transverse-transverse diagram indicates that the contribution from higher angular momentum states is small there. Results obtained by Donoghue and Gomm⁷ also found that contributions due to higher angular momentum states were small.

The final result for the sum of the transverse-transverse box diagram and the transverse-transverse crossed box diagram is,

$$\begin{aligned} E_{TT} &= TTBOX + TTCROSS = -(.089 \pm .018) \alpha_c^2 (T_i \cdot T_j)^2 / R \delta_{S,0} \\ &\quad - (.0098 \pm .002) \alpha_c^2 (T_i \cdot T_j)^2 / R \delta_{S,1} \\ &\approx -.0098 \alpha_c^2 (T_i \cdot T_j)^2 (\sigma_i \cdot \sigma_j)^2 / R \end{aligned}$$

within the accuracy stated. Comparing the magnitude of the fourth order result with that of the second order result,

$$E_{TT}/E_2 \approx .055 \alpha_c |T_i \cdot T_j| |\sigma_i \cdot \sigma_j|$$

Or, E_{TT} varies from

$$E_{TT} \approx .08 E_2 \quad \text{for spin 1 mesons,}$$

to

$$E_{TT} \approx .44 E_2 \quad \text{for spin 0 mesons.}$$

The result for the sum of the mixed coulomb-transverse diagrams must be multiplied by two since the reverse of the diagrams contributes an equal result. After multiplying by this factor of two we find,

$$\begin{aligned} E_{CT} = 2(CTBOX + CTCROSS) &= -(0.020 \pm .01) \alpha_c^2 (T_i \cdot T_j)^2 / R \delta_{S,0} \\ &\quad - (0.0085 \pm .0026) \alpha_c^2 (T_i \cdot T_j)^2 / R \delta_{S,1} \\ &\approx -0.0076 \alpha_c^2 (T_i \cdot T_j)^2 |\sigma_i \cdot \sigma_j| / R \end{aligned}$$

within the specified error.

Finally we write the result for the coulomb-coulomb box diagram,

$$\begin{aligned} E_{CC} &= (.11 \pm .026) \alpha_c^2 (T_i \cdot T_j)^2 \delta_{S,0} / R \\ &\quad + (.085 \pm .017) \alpha_c^2 (T_i \cdot T_j)^2 \delta_{S,1} / R \\ &\approx .0975 \alpha_c^2 (T_i \cdot T_j)^2 / R \end{aligned}$$

We find that, just as in the second order case, the pure coulomb interactions do not produce a spin dependent mass splitting.

Final expressions for the above terms can be written as,

$$E_{TT} = -.16\alpha_c^2 (T_i \cdot T_j)^2 (S_i \cdot S_j)^2 / R$$

$$E_{CT} = -.03\alpha_c^2 (T_i \cdot T_j)^2 |S_i \cdot S_j| / R$$

$$E_{CC} = .0975\alpha_c^2 (T_i \cdot T_j)^2 / R$$

And the result for E_2 is,

$$E_2 = -.708 (T_i \cdot T_j) (S_i \cdot S_j) / R$$

We use the values of R , B , and Z_0 obtained from the second order calculation to compute the fourth order energy shifts. The values of R for the π , ρ , N , and Δ are:

$$R_{\pi}=3.34 \text{ GeV}^{-1}, R_{\rho}=4.71 \text{ GeV}^{-1}, R_N=5 \text{ GeV}^{-1}, R_{\Delta}=5.48 \text{ GeV}^{-1}$$

The old value $\alpha_c=2.2$ was obtained by fit to the N - Δ mass splitting using only the second order calculation. Now also including the fourth order splittings that we have calculated, we should refit α_c so that the N - Δ mass splitting is still 300 MeV. Thus,

$$300 \text{ MeV} = 300 \text{ MeV} (\alpha_{\text{new}}/\alpha_{\text{secondorder}}) +$$

$$44 \text{ MeV} (\alpha_{\text{new}}/\alpha_{\text{secondorder}})^2$$

This implies that $\alpha_{\text{new}} \approx .89\alpha_{\text{secondorder}} \approx 1.96$. We now use α_{new} to calculate the mass splitting to fourth order. The results are shown in Table 5-1.

Table 5-1				
Fourth order mass shifts in MeV				
Particle	E_{TT}	E_{CT}	E_{CC}	E_A
π	-184	-46	199	-31
ρ	-15	-11	141	115
N	-51	-8	100	41
Δ	-9	-7	91	75

The π - ρ mass difference to second order was 503 MeV. We must multiply this result by .89 to account for the change in α_c . Therefore,

$$\Delta E_2^{\pi-\rho} = 448 \text{ MeV}$$

The fourth order result is,

$$\Delta E_4^{\pi-\rho} = 146 \text{ MeV}$$

Thus to fourth order the π - ρ mass splitting is,

$$\Delta E^{\pi-\rho} = 593 \text{ MeV}$$

in closer agreement with the experimental value of 641 MeV.

In summary, the fourth order mass splitting was found to be smaller than the second order mass splitting. Viz.,

$$(\Delta E_4/\Delta E_2)^{\pi-\rho} \approx 1/3$$

$$(\Delta E_4/\Delta E_2)^{N-\Delta} \approx 1/8$$

Also, the π - ρ mass splitting was brought closer to the experimental value. This indicates that the hadron mass splitting can be calculated perturbatively in the bag model.

We further note that the large results obtained by Donoghue and Gomm for the quark annihilation diagram are not in disagreement with the above results. They found that the major contribution to the energy shift was due to the lowest mode in the propagators. This is precisely the mode that had to be excluded in our calculation for reasons given in chapter II.

Finally, while we cannot make a definitive statement as to whether the perturbative expansion is convergent or not, we can say the fourth order results calculated here indicate it may.

Appendix A

Feynman rules for QCD in a static spherical cavity^{9,10}

(1) Draw all topologically distinct one-particle-irreducible graphs using dashed lines for coulomb gluons, wiggly lines for transverse gluons, and solid lines for quarks. Give all lines an arrow. The arrows on quark lines must be consistent throughout the graph while the arrows on gluon lines are arbitrary.

(2) Each external line carries energy (ω), radial quantum number (n), total angular momentum (J), z component (m), and orbital angular momentum (l). External quark lines are labeled with $J=j\pm 1/2$. Each loop is assigned a circulating energy (ω) and z component of angular momentum (m) consistent with conservation of ω and m at the vertices. Both ω and m are treated as *signed* quantities flowing in the direction of the arrows on all lines. Each internal line is given a total angular momentum (J). Internal transverse gluons and quark lines are further labeled with orbital angular momentum l and l' at each end. All quark lines also carry p-space indices, and all lines carry color labels in the standard fashion. Each vertex carries a radial coordinate label (r).

(3) For each vertex an integral, $\int_0^1 r^2 dr$. For each internal line a sum

over all allowed j values. For each internal or external quark or transverse gluon line, a sum over all l values consistent with j ($l=j\pm 1/2$ for quarks, $l=j-1, j, j+1$ for gluons). For each loop an integral,

$\int_{-\infty}^{\infty} d\omega/2\pi$, and a sum over all m values consistent with the current j

values. All implicit p -space and color indices summed as usual.

(4) For each internal line with its arrow pointing from a vertex labeled r' to one labeled r , l times a full partial-wave propagator:

$$\begin{aligned} \text{quarks} \quad & \sim i S_{jl} \cdot (r, r', \omega) = -i \omega^2 [\delta_{ll'} p^3 + (l'-l) p^2] f_l(\omega r) f_{l'}(\omega r') \\ & + i \omega^2 \{c_j(x) [\delta_{ll'} p^3 + (l'-l) p^2] + d_j(x) [(l'-l) p^0 \delta_{ll'} - i \delta_{ll'} p^1] \} j_l(\omega r) j_{l'}(\omega r') \end{aligned}$$

$$\text{where: } f_l(\omega r) = j_l(\omega r) \theta(r'-r) + h_l^{(1)}(\omega r) \theta(r-r')$$

$$c_j(x) = [j_{j-1/2}(x) h^{(1)}_{j-1/2}(x) - j_{j+1/2}(x) h^{(1)}_{j+1/2}(x)]$$

$$\otimes [j_{j-1/2}^2(x) - j_{j+1/2}^2(x)]^{-1}$$

$$d_j(x) = i/x^2 [j_{j-1/2}^2(x) - j_{j+1/2}^2(x)]$$

$$x = \omega R$$

and $l = j+1/2$ when $l = j-1/2$ and vice versa

transverse gluons $\sim i D_{JLL'}(r, r', \omega) = -i\omega \delta_{LL'} j_L(\omega r_<) h^{(1)}_{L'}(\omega r_>)$

$$+ i\omega \left[a_j^{TM(x)} Q_{JLL'}^{TM} + a_j^{TE(x)} Q_{JLL'}^{TE} \right] j_L(\omega r) j_{L'}(\omega r')$$

where: $Q_{J,J-1,J-1}^{TM} = J+1/(2J+1)$

$$Q_{J,J-1,J+1}^{TM} = Q_{J,J+1,J-1}^{TM} = -[J(J+1)]^{1/2} / (2J+1)$$

$$Q_{J,J+1,J+1}^{TM} = J/(2J+1)$$

$$Q_{JLL'}^{TM} = 0 \text{ for all other } L, L' \text{ combination}$$

$$Q_{J,J,J}^{TE} = 1$$

$$Q_{JLL'}^{TE} = 0 \text{ for all other } L, L' \text{ combinations}$$

$$a_j^{TM(x)} = h_J^{(1)}(x) / j_J(x)$$

$$a_j^{TE(x)} = [h_J^{(1)}(x) + x h_J^{(1)'}(x)] / [j_J(x) + x j_J'(x)]^{-1}$$

coulomb gluons $\Pi \sim iG_J(r, r', \omega) = i [r_<^J (r_>)^{-(J+1)} - (rr')^J R^{-(2J+1)}]$

$$\bullet (2J+1)^{-1}$$

(5) For each external quark line entering the graph (incoming quark or outgoing antiquark), a wave function

$$\chi_l(r) = 2.27 \{ j_l(\omega_0 r) \{ \delta_{l0} - \rho^2 \delta_{l1} \} \}^{1/2}$$

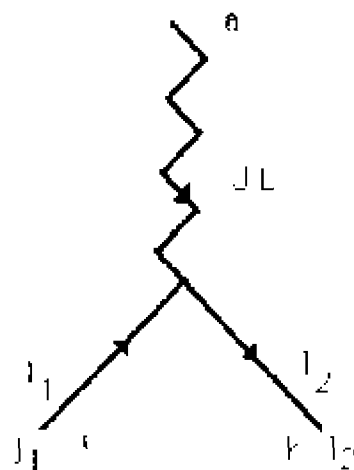
where l is summed over $l=0, 1$ and ω_0 is the energy of the quark in the 1S state.

For each external quark line leaving the graph, a factor

$$\chi_l(r) = 2.27 \{ j_l(\omega_0 r) \}^{1/2} \{ \delta_{l0} + \rho^2 \delta_{l1} \}$$

where again l is summed over 0 and 1.

(6) For every quark-transverse gluon vertex with an incoming gluon, a factor:



$$\Rightarrow g T_{j_1 j_2}^a p^2 (1/2) \gamma_{j_1 j_2}^{\mu} \vec{V}_{j_1 j_2}^{\mu} \vec{O}^{\mu} (1/2) (j_1)$$

$$(-1)^{j_2 - m_2} \begin{pmatrix} j_2 & J & j_1 \\ -m_2 & 0 & m_1 \end{pmatrix}$$

Figure A-1

Feynman rule for transverse gluon vertex function

If the gluon is outgoing replace M by $-M$ and include a factor $(-1)^{J-M-L-1}$

Where the reduced matrix element is given by:

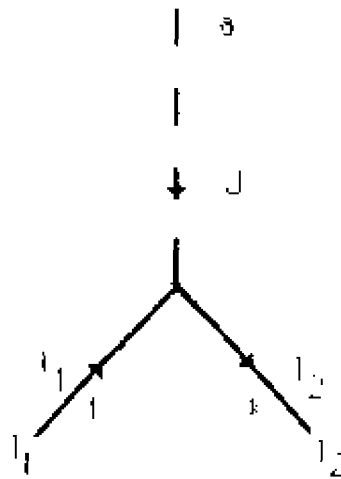
$$\begin{aligned}
 (j_2 \ 1/2 \ j_2 \parallel \sigma \parallel j_1 \ 1/2 \ j_1) &= (-1)^{j_2} \\
 &\quad \sqrt{\frac{6}{\pi}} \\
 \begin{pmatrix} j_2 & j_1 & L \\ 1/2 & 1/2 & 1 \\ j_2 & j_1 & J \end{pmatrix} &= \begin{pmatrix} j_2 & j_1 & j_1 \\ 0 & 0 & 0 \end{pmatrix}
 \end{aligned}$$

and:

$$\begin{pmatrix} j_1 & j_2 & j_3 \\ j_4 & j_5 & j_6 \end{pmatrix} = \frac{6}{\pi} (2j_1 + 1)^{1/2} \begin{Bmatrix} j_1 & j_2 & j_3 \\ j_4 & j_5 & j_6 \end{Bmatrix}$$

with a similar relation between the nine-j box and the nine-j symbol.

(7) For an quark-coulomb gluon vertex with an incoming gluon, a factor:



$$\Rightarrow ig T_{kl}^a \not{p}_2 \gamma_2 \gamma_5 \gamma_1 \not{p}_1$$

$$(-1)^{l_2 - m_2} \begin{pmatrix} l_2 & J & l_1 \\ m_2 & 0 & m_1 \end{pmatrix}$$

Figure A-2

Feynman rule for coulomb gluon vertex function

For an outgoing coulomb gluon replace M by $-M$ and include a factor $(-1)^M$.

And where:

$$(l_2, s - j_2 \| Y_1 \| l_1, s - j_1) = \frac{(-1)^{s+j_1+j_2}}{\sqrt{4\pi(2s+1)}}$$

$$\begin{pmatrix} l_2 & j_2 & s \\ j_1 & l_1 & j \end{pmatrix} = \begin{pmatrix} l_2 & j & l_1 \\ 0 & 0 & 0 \end{pmatrix}$$

Appendix B

Three-j, six-j, nine-j and reduced matrix element relations¹¹.

Relation between Clebsch-Gordan coefficients and three-j symbols

Relation B-1

$$\langle J_1 m_1 J_2 m_2 | J_1 J_2 J_3 m_3 \rangle = (-1)^{J_2 - m_2} \sqrt{\frac{2J_3 + 1}{2J_2 + 1}} \times \begin{pmatrix} J_1 & J_2 & J_3 \\ m_1 & m_2 & -m_3 \end{pmatrix}$$

Relation B-2

$$\sum_{m_1 m_2} \begin{pmatrix} J_1 & J_2 & J_3 \\ m_1 & m_2 & m_3 \end{pmatrix} \begin{pmatrix} J_1 & J_2 & J_3 \\ m_1 & m_2 & m_3' \end{pmatrix} = \frac{\delta_{J_3 J_3'} \delta_{m_3 m_3'}}{(2J_3 + 1)}$$

The three-j symbol is invariant under even permutations of the columns. For odd permutations of columns or changing the signs of all of the lower elements one must multiply by $(-1)^{J_1 + J_2 + J_3}$.

Relation B-3

$$\begin{pmatrix} l_1 & l_2 & l_3 \\ m_1 & m_2 & m_3 \end{pmatrix} \begin{matrix} l_1 & l_2 & l_3 \\ l_1 & l_2 & l_3 \end{matrix} =$$

$$\sum_{n_1, n_2, n_3} (-1)^{l_1 + l_2 + l_3 + n_1 + n_2 + n_3} \begin{pmatrix} l_1 & l_2 & l_3 \\ m_1 & n_2 & -n_3 \end{pmatrix}$$

$$\begin{pmatrix} l_1 & l_2 & l_3 \\ n_1 & m_2 & n_3 \end{pmatrix} \begin{pmatrix} l_1 & l_2 & l_3 \\ n_1 & n_2 & m_3 \end{pmatrix}$$

The six-j symbol is invariant under exchange of any columns or the exchange of any two elements from the top row with the corresponding two elements from the bottom row

8-4 The nine- j symbol

$$\left\{ \begin{array}{ccc} j_{11} & j_{12} & j_{13} \\ j_{21} & j_{22} & j_{23} \\ j_{31} & j_{32} & j_{33} \end{array} \right\} = \sum_{\text{all } m} \begin{pmatrix} j_{11} & j_{12} & j_{13} \\ m_{11} & m_{12} & m_{13} \end{pmatrix}$$

$$\begin{pmatrix} j_{21} & j_{22} & j_{23} \\ m_{21} & m_{22} & m_{23} \end{pmatrix} \quad \begin{pmatrix} j_{31} & j_{32} & j_{33} \\ m_{31} & m_{32} & m_{33} \end{pmatrix} \quad \begin{pmatrix} j_{11} & j_{21} & j_{31} \\ m_{11} & m_{21} & m_{31} \end{pmatrix}$$

$$\begin{pmatrix} j_{12} & j_{22} & j_{32} \\ m_{12} & m_{22} & m_{32} \end{pmatrix} \quad \begin{pmatrix} j_{13} & j_{23} & j_{33} \\ m_{13} & m_{23} & m_{33} \end{pmatrix}$$

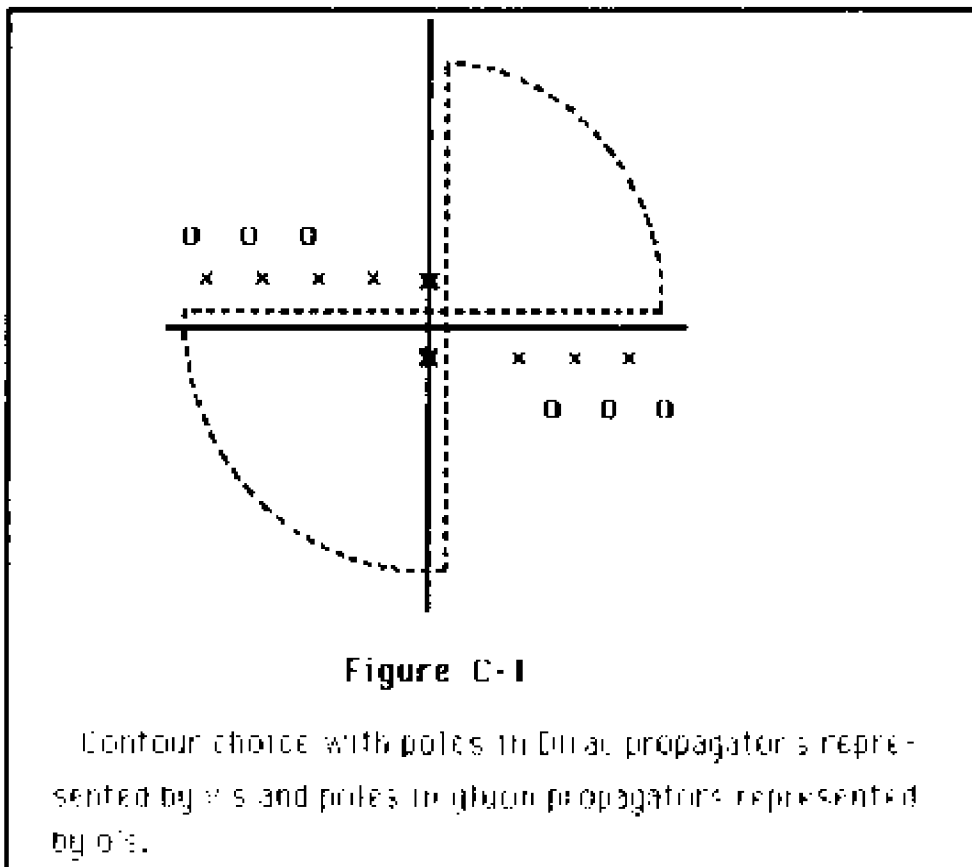
Even permutations of the nine- j symbols rows or columns leaves it unchanged. Odd permutations of the nine- j symbol changes its sign by

$$(-1)^{\text{sum of its nine elements}}$$

Appendix C

The Wick Rotation

For the Wick rotation used in Chapter IV to be valid we must show that the two quarter circles at infinity give zero contribution to the contour reproduced from Chapter IV in Figure C-1.



The terms being integrated have ω dependence only in the Dirac and transverse gluon propagators. The large ω behavior of the propagators has been obtained by Hansson and Jaffe⁹:

$$D(r,r',\omega) \approx [2\omega rr']^{-1} \{ e^{i\omega(2R-r-r')} - e^{i\omega(r_>-r_<)} \} \quad \text{for } \text{Im}(\omega) > 0$$

$$S(r,r',\omega) \approx -i[2rr']^{-1} \{ e^{i\omega(2R-r-r')} + e^{i\omega(r_>-r_<)} \} \quad \text{for } \text{Im}(\omega) > 0$$

The behavior of these propagators in the lower half of the complex ω plane is given by

$$D(r,r',\omega^*) = D^*(r,r',\omega)$$

$$S_{jll}(r,r',\omega^*) = \rho_3 S_{jll}^\dagger(r',r,\omega) \rho_3$$

Thus our proof need only be concerned with the quarter circle in the upper half of the complex ω plane.

There will always be two Dirac propagators to be integrated over but the number of transverse gluon propagators varies from zero for the coulomb-coulomb box diagram to two for the transverse-transverse box and crossed box diagrams. The transverse gluon propagator has an extra factor of ω in the denominator as compared to the coulomb gluon propagator. Therefore if we show that the quarter circle at infinity has zero contribution for CCBOX, it will also have zero contribution for the

other diagrams that have at least one extra power of ω to help with convergence.

Hence consider the ω integration of CCBOX:

$$\text{CCBOX} \approx \int d\omega dr_1 dr_2 dr_3 dr_4 r_1 r_2 r_3 r_4 e^{i\omega f(r_1, r_2)} e^{i\omega g(r_3, r_4)}$$

Where $f(r_1, r_2)$ and $g(r_3, r_4)$ are always greater than or equal to zero.

Integrating over r_1, r_2, r_3 and r_4 we find that the least well behaved part of the integral over ω is:

$$\text{CCBOX} \approx \int d\omega \omega^{-4}$$

Which vanishes for the circle at infinity. Hence we are justified in rotating the contour for all of the diagrams considered in this thesis.

Appendix D

The coulomb vertex function

The Feynman rules for QCD in a static spherical cavity listed in Appendix A were derived in the references listed. Here we give a loose derivation of the coulomb vertex factor.

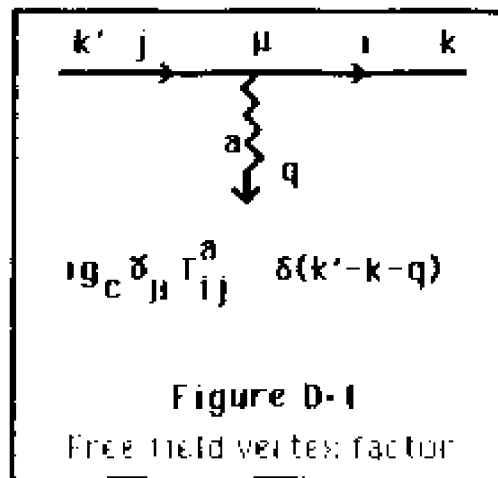
The relevant part of the QCD lagrangian density is given by

$$L = g_c \bar{\psi}_i(x) \gamma_\mu T_{ij}^a \psi_j(x) A^{\mu,a}(x)$$

First consider the second order S-matrix element for free field theory:

$$\begin{aligned} S_2 &= \langle\langle q'q' | T \int d^4x d^4y \{ i g_c \bar{\psi}_i(x) \gamma_\mu T_{ij}^a \psi_j(x) A^{\mu,a}(x) : \\ &\quad : i g_c \bar{\psi}_k(y) \gamma_\lambda T_{kl}^b \psi_l(y) A^{\lambda,b}(y) : \rangle\rangle \\ &\approx \int d^4x d^4y \{ i g_c \bar{u}_i(k) e^{ik \cdot x} \gamma_\mu T_{ij}^a u_j(k') e^{-ik' \cdot x} \} i D^{\mu\lambda}(q) e^{iq \cdot (x-y)} \\ &\quad \{ i g_c \bar{u}_k(k'') e^{ik'' \cdot y} \gamma_\lambda T_{kl}^b u_l(k''') e^{-ik''' \cdot y} \} \end{aligned}$$

We can already see what the vertex factor will be for free field theory.



Notice that since the particles were in definite states of linear momentum, an energy-momentum conserving delta function appeared at the vertex. In confined field theory the particles are in definite states of energy and angular momentum. The four dimensional integral at each vertex creates an energy and z component of angular momentum conserving delta function, but can't force conservation of all of the components of total angular momentum. This problem leads to more complex behavior at the vertex in confined field theory as will be shown below.

To simplify this problem we decompose the Dirac spinor into a direct product of $SU(2)$ spaces, ρ space and σ space, defined by

$$\begin{aligned}\gamma^0 &= \rho^3 \otimes 1 \\ \gamma^1 &= i\rho^2 \otimes \sigma^1 \\ \gamma^5 &= \rho^1 \otimes 1\end{aligned}$$

Then the wave function can be written as⁹,

$$\Psi(x) = \sum_{njl'm} \psi_{njl'm}(x) = \sum_{njl'm} \chi_{njl'l'}(r) \phi_{jl'm}(x)$$

Where l' is summed over $j \pm 1/2$ and the summation convention will be used for the rest of this Appendix.

The color factors at the vertex will not change in confined field theory so we can drop them from the remainder of this derivation and reintroduce them at the end.

Hence we can write the coulomb part of S_2 for a confined space as

$$S_2 = \langle\langle q'q' | T \int d^3x d^3y (i g_c \bar{\Psi}(x) \gamma_0 \psi(x) A^{0,a}(x) : \\ : i g_c \bar{\Psi}(y) \gamma_0 \psi(y) A^{0,b}(y) : \rangle\rangle$$

Where the integration over time has been done and turned into an energy conserving delta function at each vertex. Rewriting the above using the SU(2) decomposition scheme and inserting the propagator we find:

$$= \int d^3x d^3y (i g_c \bar{\chi}_{n j l l'}(x) \phi_{j l' m}(x) \rho^3 \chi_{n j l l'}(x) \phi_{j l' m}(x)) \\ iG(y \cdot x) (i g_c \bar{\chi}_{n j l l'}(y) \phi_{j l' m}(y) \rho^3 \chi_{n j l l'}(y) \phi_{j l' m}(y))$$

Where the coulomb gluon propagator has been derived by T. D. Lee¹⁰ to be:

$$G(y-x) = \sum_{LM} |2L+1|^{-1} [r_<^L r_>^{-(L+1)} - (xy)^L R^{-(2L+1)}] Y_{LM}(y) Y_{LM}^*(x)$$

We switch to a coordinate free representation for the spinor spherical harmonics:

$$\phi_{jm}(x) = \langle\langle x | 1/2 j m \rangle\rangle$$

Then examining only the vertex at x where the gluon **leaves** the vertex we have:

$$\begin{aligned} \text{Vertex} &= igT_{ij}^a \int_0 dr r^2 \int dx \langle\langle J 1/2 j m | x \rangle\rangle Y_{J,M}^*(x) \langle\langle x | J 1/2 j m \rangle\rangle \\ &= igT_{ij}^a (-1)^M \int_0 dr r^2 \langle\langle J 1/2 j m | Y_{J,-M} | J 1/2 j m \rangle\rangle \end{aligned}$$

Applying the Wigner-Eckart theorem:

$$\text{Vertex} = igT_{ij}^a (-1)^M (-1)^{j-m} \begin{pmatrix} j & J & 1/2 \\ -m & -M & m \end{pmatrix}$$

$$\langle\langle J 1/2 j || Y_J || J 1/2 j \rangle\rangle \int_0 dr r^2$$

which is the vertex function for an outgoing gluon. Note that for an incoming gluon we wouldn't have the factor $(-1)^M$ and instead of the $-M$ in the three- j symbol, we would have an M in agreement with the Feynman rules found in Appendix A.

Footnotes

1. Gell-Mann, M., Phys. Lett. 8, 214 (1964)
Zweig, G., CERN Report 8182/TH.401
Zweig, G., CERN Report 8419/TH.412, reprinted in Developments in the Quark Theory of Hadrons, vol. 1: 1964-1978, ed. D. B. Lichtenberg and S. P. Rosen (Hadronic Press, Nonantum, Mass., 1980), p.22
2. Greenberg, O. W., Phys. Rev. Lett. 13, 598 (1964)
3. See for example: Marciano and Pagels, Physics Reports C 36, 137 (1978)
4. Politzer, H. D. Phys. Rev. Lett. 30, 1346 (1973)
Gross, D. J. and Wilczek, F., Phys. Rev. Lett. 30, 1343 (1973)
Gross, D. J. and Wilczek, F., Phys. Rev. D8, 3633 (1973)
5. A. Chodos, R.L. Jaffe, K. Johnson, C. B. Thorn, and V. F. Weisskopf, Phys. Rev. D 9, 3471 (1974)
A. Chodos, R.L. Jaffe, K. Johnson, and C. B. Thorn, Phys. Rev. D 10, 2599 (1974)

6. T. De Grand, R. L. Jaffe, K. Johnson, and J. Kiskis, *Phys. Rev. D* 12, 2060 (1975)
7. Donoghue, J. F. and Gomm, H. *Phys. Rev. D* 28, 2800 (1983)
8. T. D. Lee, *Phys. Rev. D* 19, 1802(1979)
9. T. H. Hansson and R. L. Jaffe, *Phys. Rev. D* 28, 882 (1983)
10. A. R. Edmonds, *Angular Momentum in Quantum Mechanics*, 2nd ed. (Princeton University Press, N.J., 1960)

VITA

Timothy John Havens

Born in Bismarck, North Dakota, February 1, 1956 to Harold and Luanne Havens. Graduated from Orting High School in Orting, Washington in June of 1974. A Bachelor of Science degree was obtained in 1980 from Eckerd College in St. Petersburg, Florida. Received a Master of Science from The College of William and Mary in Williamsburg, Virginia in 1981.

The author has accepted a faculty appointment with Francis Marion College in Florence South Carolina.